~~RESTRICTED~~

NACA

RESEARCH MEMORANDUM

EFFECT OF AIR DISTRIBUTION ON RADIAL TEMPERATURE DISTRIBUTION

IN ONE-SIXTH SECTOR OF ANNULAR TURBOJET COMBUSTOR

By Herman Mark and Eugene V. Zettle

Lewis Flight Propulsion Laboratory
Cleveland, Ohio

AFMDC
TECHNICAL LIBRARY
AFL 2811

NATIONAL ADVISORY COMMITTEE
FOR AERONAUTICS

WASHINGTON
April 5, 1950

~~RESTRICTED~~

319.98/13

Space Administration

Langley Research Center
Hampton, Virginia
23665

JUN 1 6 1983

Reply to Attn of   139A

TO: Distribution

FROM: 180A/Security Classification Officer

SUBJECT: Authority to Declassify NACA/NASA Documents Dated Prior to
          January 1, 1960

(informal, correspondence)

Effective this date, all material classified by this Center prior to
January 1, 1960, is declassified. This action does not include material
derivatively classified at the Center upon instructions from other Agencies.

Immediate re-marking is not required; however, until material is re-marked by
lining through the classification and annotating with the following statement,
it must continue to be protected as if classified:

   "Declassified by authority of LaRC Security Classification Officer (SCO)
   letter dated June 16, 1983," and the signature of person performing the
   re-marking.

If re-marking a large amount of material is desirable, but unduly burdensome,
custodians may follow the instructions contained in NHB 1640.4, subpart F,
section 1203.604, paragraph (h).

This declassification action complements earlier actions by the National
Archives and Records Service (NARS) and by the NASA Security Classification
Officer (SCO). In Declassification Review Program 807008, NARS declassified
the Center's "Research Authorization" files, which contain reports, Research
Authorizations, correspondence, photographs, and other documentation.
Earlier, in a 1971 letter, the NASA SCO declassified all NACA/NASA formal
series documents with the exception of the following reports, which must
remain classified:

Document No.	First Author
E-51A30	Nagey
E-53G20	Francisco
E-53G21	Johnson
E-53K18	Spooner
SL-54J21a	Westphal
E-55C16	Fox
E-56H23a	Himmel

JUN 2 3 1983

If you have any questions concerning this matter, please call Mr. William L. Simkins at extension 3281.

Jess G. Ross

Jess G. Ross
2898

Distribution:
SDL 031

cc:
NASA Scientific and Technical
    Information Facility
P.O. Box 8757
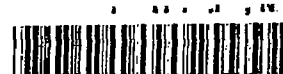BWI Airport, MD 21240

NASA--NIS-5/Security
180A/RIAD
139A/TU&AO
139A/WLSimkins:elf 06/15/83 (3281)

139A/JS 6-15-83

31-01 HEADS OF ORGANIZATIONS
HESS, JANE S.
MAIL STOP 185   BLDG 1194

0069251

~~RESTRICTED~~

NATIONAL ADVISORY COMMITTEE FOR AERONAUTICS

RESEARCH MEMORANDUM

EFFECT OF AIR DISTRIBUTION ON RADIAL TEMPERATURE DISTRIBUTION

IN ONE-SIXTH SECTOR OF ANNULAR TURBOJET COMBUSTOR

By Herman Mark and Eugene V. Zettle

SUMMARY

As part of a program conducted to determine a method of con-
trolling radial exhaust-gas-temperature distribution in a gas-
turbine combustion chamber, an experimental investigation was made
in a one-sixth sector of an annular turbojet combustor. A partic-
ular design method of controlling the radial variation of the com-
bustor exhaust-gas temperature was studied. The method chosen
consisted in adjusting the radial distribution of secondary or
dilution air entering the combustion zone. This adjustment was
achieved by one or both of two methods: (1) by ducting the dilu-
tion air into the combustion zone in a predetermined manner through
hollow radial struts, or (2) by modifying the basket-wall open-hole
area.

The combustor modifications investigated consisted of combi-
nations of design modifications in three principal sections of the
combustor: (1) the primary-zone basket wall, (2) the secondary-
zone basket wall, and (3) the hollow radial struts. The results
of an experimental investigation of 16 separate combinations of
such design modifications indicated that in this combustor secondary-
zone basket-wall modifications have a large effect on the radial
distribution of exhaust-gas temperatures. Modifications in the
secondary-zone basket walls must be accompanied by a suitable
primary-zone basket-wall design, however, to make possible actual
control of the exhaust-gas radial temperature distribution. A
suitable primary-wall design in the combustor under consideration
consisted of a primary-zone basket wall, which provided alternate
fuel-rich and air-rich sectors longitudinally along the combustor.
Modifications of the hollow radial struts for ducting dilution air
into the combustion zone have some effect on the exhaust-gas radial
temperature distribution. For the combustor investigated herein,
this method does not make possible complete control of the exhaust-
gas radial temperature distribution. Each row of such hollow radial
struts resulted in combustor pressure losses approximately double
those of a combustor without struts.

~~RESTRICTED~~

INTRODUCTION

For each gas-turbine design, a turbine-inlet-temperature distribution exists that will allow maximum blade strength and maximum blade life at the operating temperatures. Maintenance of a proper temperature distribution at the combustor outlet is therefore desirable.

As part of the combustion research program being conducted at the NACA Lewis laboratory, an experimental investigation was made in a one-sixth sector of an annular turbojet combustor. The investigation was conducted to study a design method of controlling the radial variation of the gas temperatures at the combustor outlet. The method consisted in varying the radial distribution of dilution air entering the combustion zone by modifying the design of the basket wall or by introducing the air through hollow radial struts.

The performance of a combustor designed to control the radial distribution of dilution air entering the combustion zone was determined and then the combustor was redesigned in an attempt to improve performance. The performance of each new design was investigated and the information obtained was used in determining the next design. The most important standard of performance in such an investigation was, of course, the outlet-temperature distribution. In redesigning the combustor, however, all the principal performance characteristics were considered. For most of the modifications, these characteristics included the altitude operating limits, the combustor total-pressure loss, and the combustion efficiency. In some cases, investigation of all the performance characteristics was considered unnecessary if one or the other of the characteristics already determined was extremely undesirable. No attempt was made to show or to discuss all the modifications that were investigated. Performance data are presented for 16 combustor designs illustrating some of the factors that must be considered in attempting to control radial temperature distribution at the outlet of a gas-turbine combustor.

APPARATUS

Installation

A schematic diagram of the installation is shown in figure 1. Combustion air was supplied to the setup from the laboratory air-supply system at pressures up to 55 pounds per square inch absolute. The laboratory exhaust system removed the exhaust gases and could maintain pressures as low as 2 pounds per square inch absolute within the combustion chamber.

A gasoline-fired air preheater was located upstream of the setup in a bypass to control combustor-inlet temperatures. The quantity of air flowing through the bypass, the total air flow, and the combustion-chamber pressure were regulated by three remote-control valves.

Two quartz observation windows were installed in the side wall of the combustion chamber for visual inspection of combustion during operation.

Instrumentation

The inlet-air temperatures were measured at station 1 (fig. 1) by means of three iron-constantan thermocouples (fig. 2(a)) evenly spaced across the duct. Rakes of chromel-alumel thermocouples (figs. 2(b) and 2(d)) were used at stations 2 and 3 (fig. 1) for measuring the exhaust-gas temperatures. Five rakes of thermocouples were placed at station 2 spaced at 10° intervals across the duct. Each rake contained five thermocouples located at the centers of equal areas of the cross section. At station 3 two such rakes were used to check for afterburning. All thermocouples were connected to calibrated potentiometers. Static and total pressures were measured at stations 1 and 3 by means of static wall taps and impact-tube rakes (figs. 2(c) and 2(d)) connected to 84-inch water and mercury manometers, which were photographed to reduce the time of operation at each test condition. Air flow was metered through a Daniel's concentric-hole orifice and fuel flow was metered by calibrated rotameters. The fuel used was AN-F-48b.

Combustors

The combustor, which was a one-sixth sector of an annular turbojet combustor, consisted of the combustor outer housing, the fuel manifold, four fuel-injection nozzles (capacity, 10.5-gal/hr and 60°-hollow-cone spray at pressure differential of 100 lb/sq in.), and the internal air baffles referred to hereinafter as the "basket." The upstream and the downstream halves of the basket were arbitrarily designated the primary-zone and secondary-zone walls, respectively.

Each of the combustor baskets investigated is designated by a series of numbers and letters, for example, the initial basket is designated $1-1B_1$. (See fig. 3(a)). The series of numbers and letters by which a basket is identified serves as a code in which

the first number (1 or 2) refers to the primary-wall design, and the
second number (1, 2, or 3) refers to the secondary-wall design. The
letter indicates the type of dilution-air radial distribution that
the geometry of the slot opening on the face of the struts was
intended to induce. The slots used were:

A, slot opening designed to induce a shift in the radial dis-
tribution of dilution air toward the turbine-blade tip

B, slot opening designed to induce equal flow through the struts
at blade tip and root

C, slot opening designed to induce a shift in the radial dis-
tribution of the dilution air towards the blade root

The subscript 1 or 2 indicates the design group of the hollow
radial struts, which are used to distribute the dilution air.

Combustor designs having common primary- and secondary-wall
designs and differing only in type of radial air-flow distribution,
which the design is intended to produce because of the type of strut
used (A, B, or C), conveniently fall into series. The various series
of baskets are subsequently described in the order they were designed
and investigated.

Series 1-1( )$_1$. - The development of the inner and outer walls
of initial combustor basket 1-1B$_1$ (fig. 3(a)) is shown in figure 4(a).
Primary-wall design 1 used in this basket was that of a contemporary
no-strut type with a row of thin louvers added downstream of each row
of holes. Secondary-wall design 1 used in this basket was intended to
control the radial distribution of the secondary air. The design
consisted of two rows of large circular holes in the outer wall of
the basket connected to two rows of rectangular, round-corner holes
in the inner wall by means of slotted radial struts. These two rows
of struts were staggered. The secondary air passed through the holes
in the basket walls, the hollow radial struts, and the slots into the
combustion zone. The slots were faced upstream so that the secondary
air turning downstream would cool the struts. The B$_1$ struts in the
initial basket 1-1B$_1$ had slots of uniform width (cutaway portion of
fig. 3(a)) and were intended to induce a uniform air distribution.
Strut series 1 (A$_1$, B$_1$, and C$_1$) is shown in the insert in fig-
ure 3(a).

1193

The other baskets in this series ($1\text{-}1A_1$ and $1\text{-}1C_1$) were the same as the initial basket except that they had the A_1 and C_1 struts, respectively, instead of the B_1 struts used in basket $1\text{-}1B_1$.

Series $1\text{-}2(\ )_1$. - Basket $1\text{-}2B_1$ is shown in figure 3(b) and a development of its inner and outer walls is shown in figure 4(b). The baskets of series $1\text{-}2(\ )_1$ were the same as those of series $1\text{-}1(\ )_1$ except for a difference in the secondary-wall design. Secondary-wall design 1 was modified by removing the upstream row of radial struts and changing the remaining holes to rectangular shape. The resultant design is designated secondary-wall design 2 and is shown as the shaded portion of figure 4(b).

Baskets $1\text{-}2A_1$ and $1\text{-}2C_1$ were the same as basket $1\text{-}2B_1$ except that they had A_1 and C_1 struts, respectively.

Series $2\text{-}2(\ )_1$ and $2\text{-}2(\ )_2$. - Basket $2\text{-}2B_1$, which is shown in figure 3(c), has primary-wall design 2 (shaded region in fig. 4(c)). The open area in the basket wall upstream of the row of struts consisted of long thin triangular slots running axially along the length of the basket wall. The slots were staggered with respect to the fuel-injection nozzles to give alternate fuel-rich and air-rich sectors running the length of the primary zone. This alternation allowed optimum fuel-air ratios to exist at the interface between each fuel-rich and its adjacent air-rich sector all along the length of the zone. The A_1 and C_1 struts (fig. 3(a)) were substituted in this basket design to produce basket modifications $2\text{-}2A_1$ and $2\text{-}2C_1$. Struts of series 2 (A_2, B_2, and C_2) are shown in figure 3(c). The B_2 strut is the same as the B_1 strut. Baskets of series $2\text{-}2(\ )_2$ were obtained by substituting struts of series 2 in the basket shown in figure 3(c).

Series $2\text{-}3(\ )_2$ and Basket $2\text{-}3C_0$. - Basket $2\text{-}3B_2$, which is shown in figure 3(d), has secondary-wall design 3, shown as the shaded region in figure 4(d). The secondary-wall design is the same as secondary-wall design 2 except that the rectangular holes in the outer wall of the basket have been eliminated and an additional row of rectangular openings has been added in the inner basket wall. This row of holes is in the downstream end of what is arbitrarily called the primary zone but the row is named a secondary-wall modification because it is intended to introduce dilution air into the combustion zone. Strut series 2 was used in conjunction with

primary-wall design 2 and secondary-wall design 3 to give basket series 2-3( )$_2$. Basket 2-3C$_0$ is the same as any basket in series 2-3( )$_2$ but with the row of radial struts removed.

The basket designs investigated are summarized in figure 5.

PROCEDURE

The combustor-inlet and -outlet conditions required to simulate zero-ram operation in a reference turbojet engine at various altitudes and engine speeds are shown in figure 6. The data of figure 6 were obtained from reference 1. With each combustor basket, some or all the performance characteristics were investigated as described in the following paragraphs.

Temperature distribution. - The combustor-outlet-temperature distribution was determined with combustor-inlet conditions simulating zero-ram operation of the reference engine at an altitude of 40,000 feet, rated engine speed (17,400 rpm), and a fuel-air ratio of 0.016. Rated engine speed was chosen because the highest combustor-outlet temperatures are required at rated speed and any difficulties due to improper temperature distribution will therefore be most severe at this condition. A fuel-air ratio of 0.016 was used because with 100-percent combustion efficiency it approximately gives the average combustor-outlet temperature required for operation of the reference engine at the simulated-flight condition.

Temperature-rise efficiency. - The variation of temperature-rise efficiency with fuel-air ratio was determined at combustor-inlet conditions simulating rated engine speed at an altitude of 40,000 feet over a range of fuel-air ratios extending from 0.015 to 0.020 or to a fuel-air ratio giving local thermocouple readings above 2000° F, whichever occurred first.

Total-pressure loss. - Simultaneously with the determination of temperature distribution and temperature-rise efficiency, total pressures at the inlet and the outlet of the combustor were measured and recorded. The difference between the inlet and outlet total pressures was considered to be the average loss in total pressure through the combustor.

Altitude operating limits. - The altitude operating limits were determined over a range of simulated engine speeds from 50- to 100-percent rated engine speed. The method used to determine the altitude operating limits is described in reference 2. Investigations at lower engine speeds were impossible at the altitudes considered because of limitations of the laboratory air supply.

RESULTS AND DISCUSSION

In the following paragraphs, the results shown in figure 7 to
12 are discussed in detail and are in the same order as the basket
modifications appear in figure 5.

Series 1-1( )$_1$

Temperature distribution. - The radial-temperature distribution
at the combustor outlet for the various baskets investigated is
presented for combustor-inlet-air conditions simulating an altitude
of 40,000 feet and an engine speed of 17,400 rpm. Each symbol on
the radial-temperature-distribution curves represents the average of
five circumferential temperature readings at the given radial dis-
tance from the turbine-root section in the engine. (See fig. 2(b)
for instrumentation.) The curves therefore show the average radial
temperature distribution for a given modification. The radial
temperature distributions obtained with each of the baskets of
series 1-1( )$_1$ are presented in figure 7(a). Basket 1-1A$_1$ gave a
temperature distribution increasing from blade tip to root. Baskets
1-1B$_1$ and 1-1C$_1$ also gave this same type of distribution; however,
the effects of the dilution-air distributing struts are in evidence.

The temperature distribution of series 1-1( )$_1$ at a different
set of operating conditions (altitude, 30,000 ft; engine speed,
17,400 rpm) is shown in figure 7(b). The distributions for the
baskets in series 1-1( )$_1$ at these conditions were not the same as
the distributions for these baskets at the operating conditions of
figure 7(a). The dissimilarity illustrates that the temperature
distribution is unpredictable for this series with changes in
operating conditions.

Temperature-rise efficiency. - The temperature-rise efficiencies
for these basket modifications are shown in figure 7(c). The effi-
ciencies for all the baskets of this series are below 90 percent at
all fuel-air ratios investigated and decrease markedly with increase
in fuel-air ratio.

Total-pressure loss. - In order to make comparisons with total-
pressure losses of other turbojet combustors, the total-pressure
loss through the combustor sector is expressed as $\Delta P_T/q_r$ (where
ΔP_T is the actual total-pressure loss and q_r is the dynamic pres-
sure that would exist at the inlet section if the velocity at that

section were based on the maximum cross-sectional area of the combustor housing). The ratio of the total-pressure loss to the reference dynamic pressure $\Delta P_T/q_r$ expressed as a function of inlet-to-outlet density ratio ρ_1/ρ_2 is presented in figure 7(d) for basket series 1-1( )$_1$. The values of $\Delta P_T/q_r$ are approximately the same for each of the three baskets. The average value of $\Delta P_T/q_r$ is approximately 63 at a density ratio of 2.5. This value is about 3.5 times as large as for a contemporary no-strut-type basket.

Altitude operating limits. - The altitude operating limits of each of the three baskets of this series are shown in figure 7(e). For comparison, the operating limits for a contemporary no-strut-type basket are also presented. The operating limits for the combustors of this series are higher at low engine speeds but much lower at high engine speeds than the operating limits for the reference combustor. The low operating limits at high engine speeds were due to insufficient temperature rise through the combustor. This insufficiency was caused by both the decrease in temperature-rise efficiency with increase in fuel-air ratio, as shown in figure 7(c), and by the high values of temperature rise that are required for engine operation at high speeds, as shown in figure 6. The attainable temperature rise was probably limited for two reasons: (1) The primary zone was fuel rich at the higher over-all fuel-air ratio, making it necessary for combustion to begin farther downstream in the combustor. This necessity was confirmed by visual observations showing that the flame seat moved farther downstream as the fuel-air ratio was progressively increased. (2) The intense radial penetration of the dilution air due to the double row of struts quenched the reaction processes at the location of the struts, thereby giving too short a distance for complete combustion at high fuel-air ratios.

Summary. - The baskets of series 1-1( )$_1$ gave low temperature-rise efficiencies at high fuel-air ratios, high pressure losses, and very low altitude operating limits at high engine speeds. In addition, although the combustor-outlet-temperature distribution was influenced by changing the radial distribution of dilution air by means of radial struts, the temperature distributions for the various baskets were not reproduced at different inlet-air conditions.

Series 1-2( )$_1$

Temperature distribution. - The radial temperature distribution at the combustor outlet obtained with baskets of series 1-2( )$_1$

(fig. 8(a)) show temperatures increasing from blade tip to root over
the principal portion of the combustor cross section regardless of
the type of strut used. In figure 8(b) are shown temperature-
distribution profiles for the individual thermocouple rakes at each
circumferential station for modification $1-2C_1$. When these curves
are compared with the average profile curve for basket $1-2C_1$ from
figure 8(a), the curves at the individual stations do not, in gen-
eral, have the same shape as the average profile. This trend is
representative of almost all the temperature profiles for baskets
in which primary zone 1 was used. The single profile curve for
each basket, as shown in figure 8(a), is the average of the five
individual rake profiles (fig. 8(b)). Additional data not included
herein showed that the temperature-distribution patterns again
varied considerably with changes in engine operating conditions.

Temperature-rise efficiency. - Temperature-rise efficiencies
were investigated for only one ($1-2C_1$) of the three baskets of this
series and are shown in figure 8(c). The efficiency again decreases
with increase in fuel-air ratio but not as sharply as for basket
$1-1C_1$. From this relation, it can be reasoned that the decrease in
quenching by the dilution air (obtained by changing from secondary-
wall design 1 to secondary-wall design 2) is in itself insufficient
to give the necessary increase in combustion efficiency at high
fuel-air ratios.

Total-pressure loss. - The average value of $\Delta P_T/q_r$ at a
density ratio of 2.5 was about 33 (fig. 8(d)). The pressure losses
for these baskets are therefore about one-half as great as for
baskets of series $1-1(\ )_1$.

Altitude operating limits. - The operating limits were deter-
mined for only one of the baskets ($1-2C_1$), as shown in figure 8(e),
and are somewhat higher than those obtained with the baskets of
series $1-1(\ )_1$. The decrease in the quenching effect of the dilu-
tion air has therefore been partly effective in raising the oper-
ating limits at high fuel-air ratio. The flame seat was again
observed to move farther downstream as the fuel-air ratio was
progressively increased.

Summary. - The baskets of series $1-2(\ )_1$ gave lower pressure
losses and higher operating limits at high engine speeds than did
the baskets of series $1-1(\ )_1$. No combustor-outlet radial-
temperature-distribution control was affected by changes in the
radial distribution of the dilution air.

Series 2-2( )$_1$ and 2-2( )$_2$

Temperature distribution. - When the primary-zone-wall design
was modified in an attempt to produce continuous fuel-rich and air-
rich sectors in the primary region (series 2-2( )$_1$), the temperature-
distribution curves (fig. 9(a)) still showed temperatures increasing
from blade tip to root over the principal portion of the combustor
cross section regardless of the strut configuration used.

The temperature distribution of series 2-2( )$_1$ at a different
set of operating conditions (altitude, 30,000 ft; engine speed,
17,400 rpm) is shown in figure 9(b). The distributions of outlet
temperatures for the baskets in series 2-2( )$_1$ at these operating
conditions were similar to the distributions for these baskets at
the operating conditions in figure 9(a). The similarity illustrates
that the temperature distributions for this series were more repro-
ducible for changes in operating conditions than were the temperature
distributions for series 1-1( )$_1$ and 1-2( )$_1$.

In figure 9(c) are shown temperature-distribution profiles for
the individual thermocouple rakes at each circumferential station
for basket 2-2C$_1$. When these curves are compared with the average
profile curve for basket 2-2C$_1$ from figure 9(a), the curves at the
individual stations have more nearly the same shape as the average
profile. This trend is representative of all the temperature
profiles for baskets in which primary zone 2 was used.

The results of modifying the strut configurations to make the
variation in the radial distributions of the dilution air more
pronounced are shown in figure 10(a) for series 2-2( )$_2$. Rede-
signing the struts so that they would have a stronger effect on the
radial distribution of the dilution air had some effect on the
radial temperature distribution, but the radial temperature dis-
tributions still increase from blade tip to root. Figure 10(b)
shows series 2-2( )$_2$ at a different set of operating conditions
(altitude, 30,000 ft; engine speed, 17,400 rpm). The distributions
of outlet temperature for baskets in series 2-2( )$_2$ at these
operating conditions were similar to the distributions for these
baskets at the operating conditions in figure 10(a).

Temperature-rise efficiency. - Temperature-rise efficiencies
for series 2-2( )$_1$ and 2-2( )$_2$ are shown in figures 9(d) and
10(c), respectively. The efficiencies, in general, remain constant
with progressive increases in over-all fuel-air ratio and show
somewhat higher values than for series 1-2( )$_1$.

1193

Total-pressure loss. - The pressure losses for series 2-2( )$_1$ and 2-2( )$_2$ are approximately the same as for series 1-2( )$_1$ (figs. 9(e) and 10(d), respectively).

Altitude operating limits. - The altitude operating limits for the baskets of these two series are presented in figures 9(f) and 10(e). All these baskets produced operating limits less than 5000 feet apart, as shown by the shaded area in the figures. The operating limits for these baskets are approximately the same at rated speed (17,400 rpm) as those for the contemporary no-strut-type basket. These operating limits are 20,000 to 30,000 feet higher at rated speed (17,400 rpm) than the limits of series 1-1( )$_1$ and 1-2( )$_1$.

The higher operating limits at rated speed and the higher combustion efficiencies at high fuel-air ratios obtained with these baskets are the result of the primary-wall design. With primary-wall design 2, the flame seat did not move downstream at high fuel-air ratios as it did with primary-wall design 1; this phenomenon was verified by visual observation through the window in the upstream end of the combustor. With the flame always seated in the extreme upstream end of the combustor, the entire combustor length was therefore always available for the combustion processes. The provision of alternate fuel-rich and air-rich sectors in the primary zone of the combustor thus proved to be highly desirable.

The success of primary-wall design 2 may possibly be attributed to one or both of the following explanations: (1) An optimum fuel-air ratio must exist somewhere in the interface between each fuel-rich and its adjacent air-rich sector all along the length of the primary zone. Continuous and unbroken longitudinal zones of optimum fuel-air ratio are thereby provided over the entire length of the primary zone greatly facilitating flame propagation in the primary zone. (2) Unpublished data obtained at the Lewis laboratory indicate that small jets of air oscillate under certain conditions when injected into a combustor similar to those described herein. The oscillation of each jet of air through small circular holes may induce instabilities in flame seating. This design, however, provides for the smooth metering of air into the chamber in continuous sectors and may therefore reduce the oscillations in the critical flame-seating regions.

Summary. - All performance characteristics were improved in this series except the pressure losses, which remained about the same as for the immediately preceding series. Changes in the radial

distribution of the dilution air by means of radial struts had some
effect on the radial temperature distribution; however, the general
trend was toward temperatures increasing from blade tip to root for
all strut designs investigated. The outlet-temperature distribution
of each of these baskets was unaltered by a change in operating con-
ditions as had occurred with the combustor baskets previously
discussed.

<center>Series 2-3( )$_2$ and Basket 2-3C$_0$</center>

Temperature distribution. - The radial temperature distribu-
tions for series 2-3( )$_2$ and basket 2-3C$_0$ are presented in fig-
ure 11(a). This figure shows the results of combining the long thin
slot primary-wall design with a rearrangement of the air-flow passage
areas in the secondary-zone walls designed to induce a temperature
distribution decreasing from blade tip to root at the combustor out-
let. The temperature distributions were regular and consistent at
various engine operating conditions and produced distributions
decreasing from blade tip to root over the principal part of the
combustor cross section regardless of the strut design used. Even
when all the struts were removed (fig. 11(a), basket 2-3C$_0$), the
principal trend of the temperature distribution remained essentially
the same. Comparison of the temperature distributions obtained with
this series of baskets with the temperature distributions obtained
with the other series of baskets shows that combustor-outlet-
temperature distribution can be controlled by variations in the air-
flow passages of the secondary-zone wall, when primary-wall design
2 (figs. 4(c) and 4(d)) is used. Such a primary design may possibly
produce more uniform temperatures in the gases entering the dilution
zone, thus facilitating radial temperature control.

Temperature-rise efficiency. - The temperature-rise efficiencies
for series 2-3( )$_2$ (fig. 11(b)) are about 10 percent higher than for
series 2-2( )$_2$ (fig. 10(c)). The efficiencies for basket 2-3C$_0$ are
of the same order of magnitude as those for series 2-2( )$_2$ and the
contemporary no-strut-type basket. All efficiencies remain approxi-
mately constant with changes in fuel-air ratio.

Total-pressure loss. - Total-pressure losses are shown in fig-
ure 11(c). At a density ratio of 2.5, series 2-3( )$_2$ has an average
$\Delta P_T/q_r$ of about 31, whereas basket 2-3C$_0$ has a $\Delta P_T/q_r$ of 18,
which is only about 30 percent of the average value of $\Delta P_T/q_r$ for
series 1-1( )$_1$.

Altitude operating limits. - The operating limits for series
2-3($)_2$ fall within the shaded region shown in figure 11(d); these
operating limits are approximately the same as those shown in fig-
ure 10(e) for the preceding series.

Summary. - The temperature-rise efficiencies and the altitude
operating limits of the baskets in series 2-3($)_2$ and 2-3C_0 compare
favorably with the efficiencies and the operating limits of the bas-
kets of series 2-2($)_1$ and 2-2($)_2$. The pressure losses for baskets
of series 2-3($)_2$ are approximately the same as those of the baskets
of series 2-2($)_2$; losses for basket 2-3C_0 are considerably lower
than those of the other basket series. The temperature distributions
for baskets of series 2-3($)_2$ and basket 2-3C_0 decreased from tip
to root. Because baskets of series 2-2($)_1$ and 2-2($)_2$ produce
temperatures increasing from tip to root, control over the radial
temperature distribution at the combustor outlet by means of basket-
wall modifications has been demonstrated. The results obtained with
the types of radial strut investigated herein show that radial struts
such as these also have some effect on the radial distribution of the
combustor-outlet temperatures.

Temperature-Contour Patterns

Isothermal contour patterns for each temperature distribution
presented herein are shown in figure 12. These patterns are typical
of the data obtained. All these contours are at the same operating
conditions and fuel-air ratio but, because of efficiency variations
from one modification to another, are at different temperature levels.
The cooling effect of the side walls and circumferential variations
in the radial temperature distributions are apparent.

Condition of Combustor Basket

During this investigation, carbon deposition was not a problem
because the combustor was operated at altitude conditions where there
is little tendency for carbon to form. No discernable carbon deposits
were noticed at any time.

Very little warping of the 16-gage Inconel basket was present
on any of the modifications. The radial struts, also fabricated
of 16-gage Inconel, showed little sign of deterioration in all but
modifications 1-1($)_1$ where some melting of the struts, or oxidation,
or both occurred.

1193

SUMMARY OF RESULTS

The following results were obtained from the experimental investigation of the performance of 16 modifications of a one-sixth sector of an annular turbojet combustor:

1. When the basic unmodified primary-wall design and hollow radial struts for ducting the dilution air into the secondary zone of the combustor were employed, the results observed were:

(a) Although the combustor-outlet-temperature distribution was influenced by changing the radial distribution of the dilution air by means of the geometry of the slots in the radial struts, the radial temperature distributions were not reproducible from one set of operating conditions to another.

(b) The observed combustor-outlet radial temperature distributions were different at each circumferential position at which temperatures were measured.

(c) Combustion efficiencies at operating conditions corresponding to an altitude of 40,000 feet and an engine speed of 17,400 rpm (rated speed) were below 90 percent and decreased markedly with increase in fuel-air ratio.

(d) The altitude operating limits were higher at simulated low engine speeds but were much lower at high engine speeds than the operating limits for the combustor without the struts.

2. Baskets with a primary-wall design that provided alternate fuel-rich and air-rich sectors longitudinally along the combustor either with or without radial struts gave the following results:

(a) The average radial temperature distribution at the combustor outlet for any one basket was reproducible from one set of operating conditions to another.

(b) The observed combustor-outlet radial temperature distributions were more nearly similar to each other at each circumferential position at which temperatures were measured.

(c) Combustion efficiencies were higher than for other baskets of this investigation.

(d) The altitude operating limits at high engine speeds were higher than for other baskets of this investigation.

NATIONAL ADVISORY COMMITTEE
FOR AERONAUTICS

1724 F Street, Northwest
Washington 25, D. C.

M.L. 278 (Monthly list of documents released by the NACA during May 1950)

Libraries in most of the important cities throughout the country, as well as libraries of schools, manufacturers, and other organizations dealing with aeronautics, are supplied copies of these publications for reference.

TECHNICAL NOTES

TN 2070   Knock-Limited Performance of Fuel Blends Containing Ethers.
           By: I. L. Drell and J. R. Branstetter.

TN 2079   Experiments in External Noise Reduction of Light Airplanes.
           By: Leo L. Beranek, Fred S. Elwell, John P. Roberts, and C. Fayette
               Taylor.

TN 2081   Correlation of Physical Properties with Molecular Structure for Dicyclic
               Hydrocarbons. I - 2-n-Alkylbiphenyl, 1,1-Diphenylalkane,
               α,ω-Diphenylalkane, 1,1-Dicyclohexylalkane, and α,ω-Dicyclohexylalkane
               Series.
           By: P. H. Wise, K. T. Serijan, and I. A. Goodman.

TN 2083   Theoretical Analysis of Various Thrust-Augmentation Cycles for Turbojet
               Engines.
           By: Bruce T. Lundin.

TN 2086   Hovering and Low-Speed Performance and Control Characteristics of an
               Aerodynamic-Servocontrolled Helicopter Rotor System as Determined
               on the Langley Helicopter Tower.
           By: Paul J. Carpenter and Russell S. Paulnock.

TN 2087   Comparison of Theoretical and Experimental Heat Transfer on a Cooled
               20° Cone with a Laminar Boundary Layer at a Mach Number of 2.02.
           By: Richard Scherrer and Forrest E. Gowen.

TN 2088   Performance and Load-Range Characteristics of Turbojet Engine in
               Transonic Speed Range.
           By: Bernard Lubarsky.

TN 2089   A Comparison of the Lateral Controllability with Flap and Plug Ailerons
               on a Sweptback-Wing Model.
           By: Powell M. Lovell, Jr. and Paul P. Stassi.

TN 2090   Investigation of Spark-Over Voltage - Density Relation for Gas-Temperature
               Sensing.
           By: Robert J. Koenig and Richard S. Cesaro.

TN 2091   Dynamics of a Turbojet Engine Considered as a Quasi-Static System.
                  By: Edward W. Otto and Burt L. Taylor, III.

TN 2093   Formulas and Charts for the Supersonic Lift and Drag of Flat Swept-
                  Back Wings with Interacting Leading and Trailing Edges.
                  By: Doris Cohen.

TN 2094   Stress-Strain and Elongation Graphs for Alclad Aluminum-Alloy
                  24S-T86 Sheet.
                  By: James A. Miller.

TN 2095   Application of the Wire-Mesh Plotting Device to Incompressible Cascade
                  Flows.
                  By: Willard R. Westphal and James C. Dunavant.

TN 2097   Improvement of High-Temperature Properties of Magnesium-Cerium
                  Forging Alloys.
                  By: K. Grube, J. A. Davis, L. W. Eastwood, C. H. Lorig, and
                       H. C. Cross.

TN 2098   The Effects of Stability of Spin-Recovery Tail Parachutes on the Behavior
                  of Airplanes in Gliding Flight and in Spins.
                  By: Stanley H. Scher and John W. Draper.

TN 2099   A Method of Calibrating Airspeed Installations on Airplanes at Transonic
                  and Supersonic Speeds by Use of Accelerometer and Attitude-Angle
                  Measurements.
                  By: John A. Zalovcik.

TN 2103   Maximum Pitching Angular Accelerations of Airplanes Measured in
                  Flight.
                  By: Cloyce E. Matheny.

TN 2106   Evaluation of Several Adhesives and Processes for Bonding Sandwich
                  Constructions of Aluminum Facings on Paper Honeycomb Core.
                  By: H. W. Eickner.

REPORTS

Rept. 924   Application of Theodorsen's Theory to Propeller Design.
                  By: John L. Crigler.
                  Formerly issued as RM L8F30.

Rept. 930   An Analytical Method of Estimating Turbine Performance.
                  By: Fred D. Kochendorfer and J. Cary Nettles.
                  Formerly issued as RM E8I16.

Rept. 931   Correlation of Cylinder-Head Temperatures and Coolant Heat Rejections of a Multicylinder, Liquid-Cooled Engine of 1710-Cubic-Inch Displacement.
By: Bruce T. Lundin, John H. Povolny, and Louis J. Chelko.
Formerly issued as RM E8B06 and RM E8B06a.

TECHNICAL MEMORANDUMS

TM 1266   Preliminary Results from Fatigue Tests with Reference to Operational Statistics.
By: E. Gassner.

TM 1270   The Gas Kinetics of Very High Flight Speeds.
By: Eugen Sanger.

TM 1275   The Solution of the Laminar-Boundary-Layer Equation for the Flat Plate for Velocity and Temperature Fields for Variable Physical Properties and for the Diffusion Field at High Concentration.
By: H. Schüh.

TM 1285   Investigations of the Wall-Shearing Stress in Turbulent Boundary Layers.
By: H. Ludwieg and W. Tillmann.

3. When a primary-wall design that provided alternate fuel-rich and air-rich sectors longitudinally along the combustor was used, the radial temperatures at the combustor outlet either increased from turbine-blade tip to root or decreased from tip to root depending on the size and the positions of the air-passage areas in the walls of the secondary zone regardless of the geometry of the slot in the hollow radial struts used.

4. More effective temperature-distribution control can be obtained in this combustor by modifications in the secondary walls than by ducting the dilution air through hollow radial struts.

5. Each row of hollow radial struts added to a combustor approximately doubled the combustor total-pressure losses.

CONCLUSION

1. A primary basket-wall design that provided alternate fuel-rich and air-rich sectors longitudinally along the combustor was amenable to outlet-temperature-distribution control.

Lewis Flight Propulsion Laboratory,
    National Advisory Committee for Aeronautics,
        Cleveland, Ohio.

REFERENCES

1. Fleming, William A.: Altitude-Wind-Tunnel Investigation of
    Westinghouse 19B-2, 19B-8, and 19XB-1 Jet-Propulsion Engines.
    I - Operational Characteristics. NACA RM E8J28, 1948.

2. Hill, Francis U., and Mark, Herman: Performance of Experimental
    Turbojet-Engine Combustor. I - Performance of a One-Eighth
    Segment of an Experimental Turbojet-Engine Combustor. NACA
    RM E7J13, 1948.
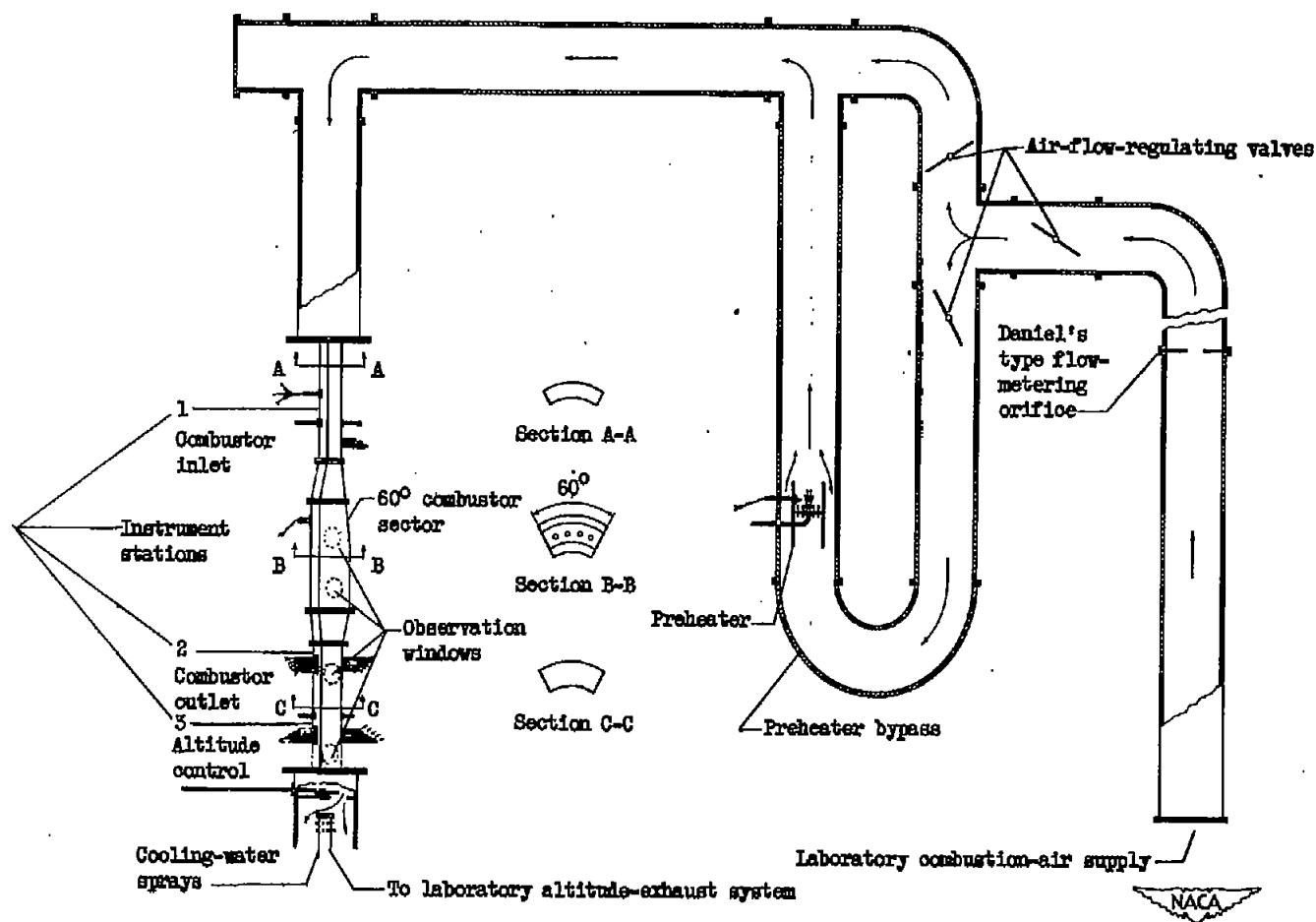
Figure 1. - Diagram of laboratory ducting and installation of one-sixth combustor sector.

(a) Iron-constantan inlet thermo-
couples, upstream at station 1.

(b) Chromel-alumel thermocouple
rakes at station 2.

(c) Inlet total-pressure rakes,
downstream at station 1.

(d) Chromel-alumel thermocouple
rakes and total-pressure
rakes at station 3.
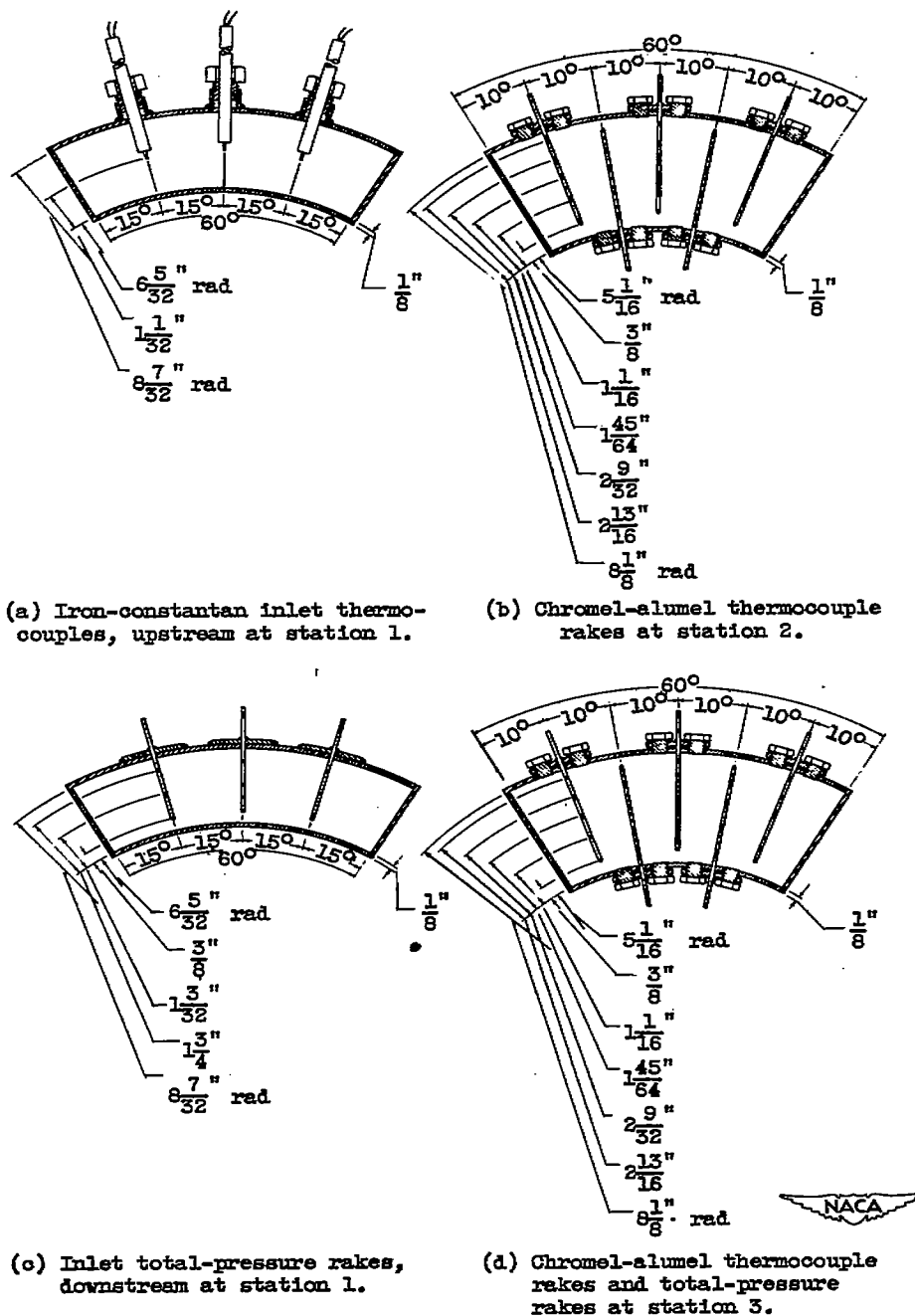
Figure 2. - Instrumentation arrangement of thermocouples and total-pressure rakes.

Strut series 1

A_1 B_1 C_1

Holes locating
fuel nozzles

(a) Series 1-1( )$_1$.

Holes locating
fuel nozzles
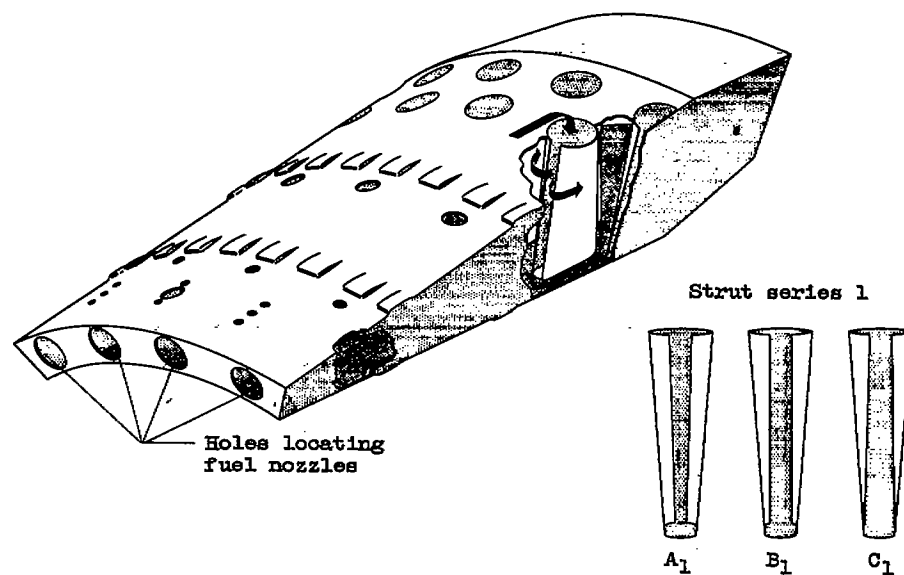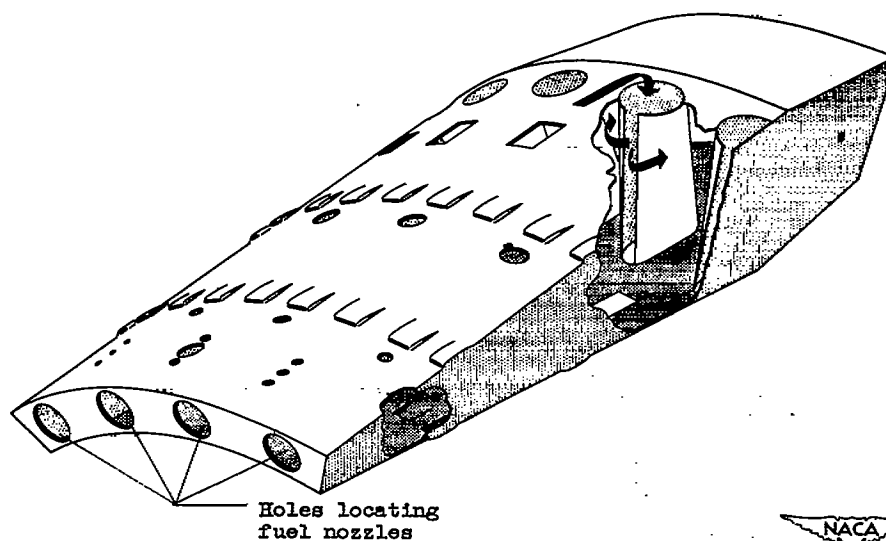
(b) Basket 1-2B$_1$.

Figure 3. - Isometric view of combustor basket illustrating basket modifications and struts.

1193

Strut series 2

Holes locating
fuel nozzles

A_2 B_2 C_2

(c) Series 2-2( )$_1$ and 2-2( )$_2$.

Holes locating
fuel nozzles

NACA
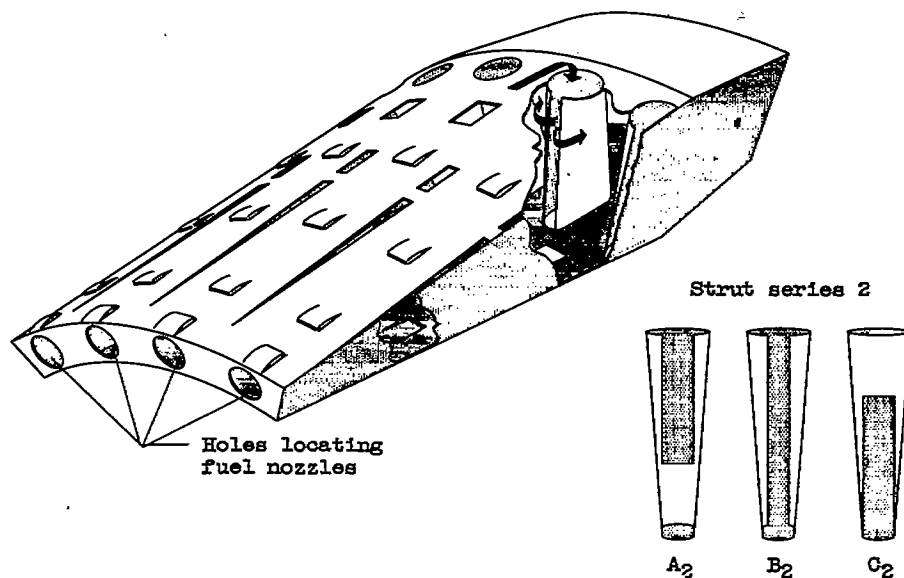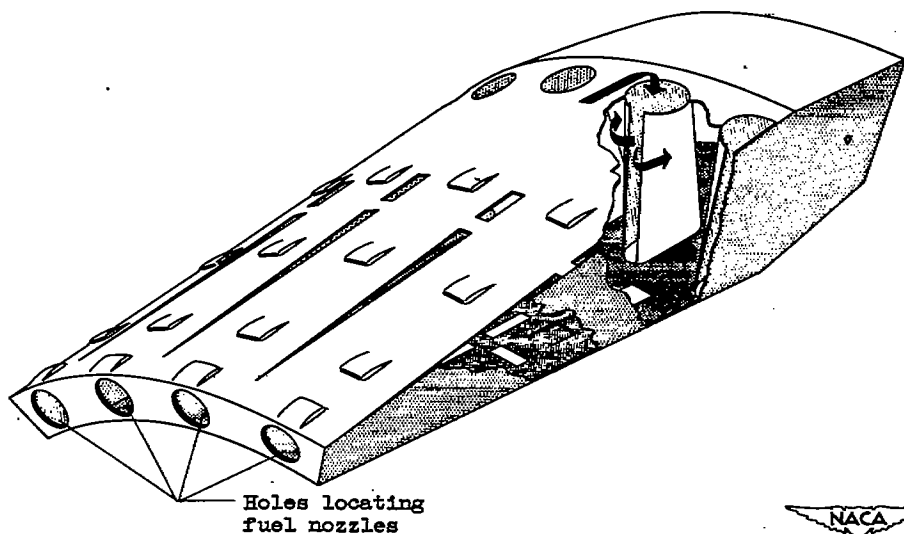
(d) Basket 2-3B$_2$.

Figure 3. - Concluded.   Isometric view of combustor basket illustrating basket modifica-
tions and struts.

240-1702-1506

Struts

Outer wall   Inner wall
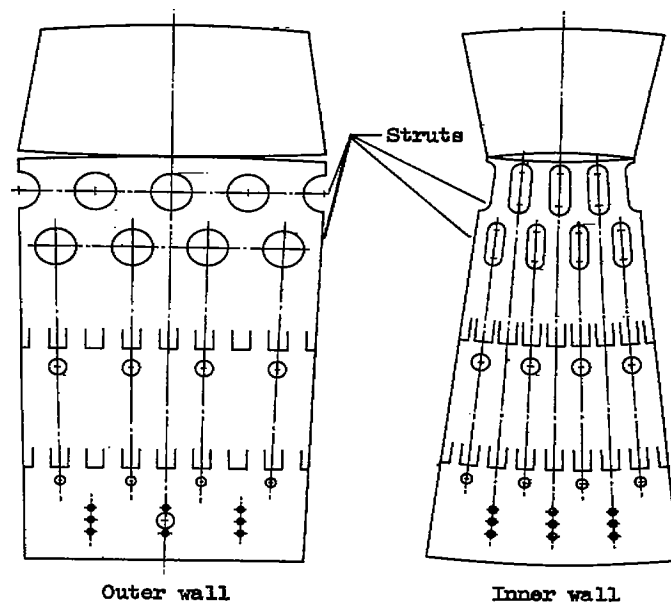
(a) Series 1-1( )$_1$; used with struts of series 1.

Struts

Outer wall   Inner wall
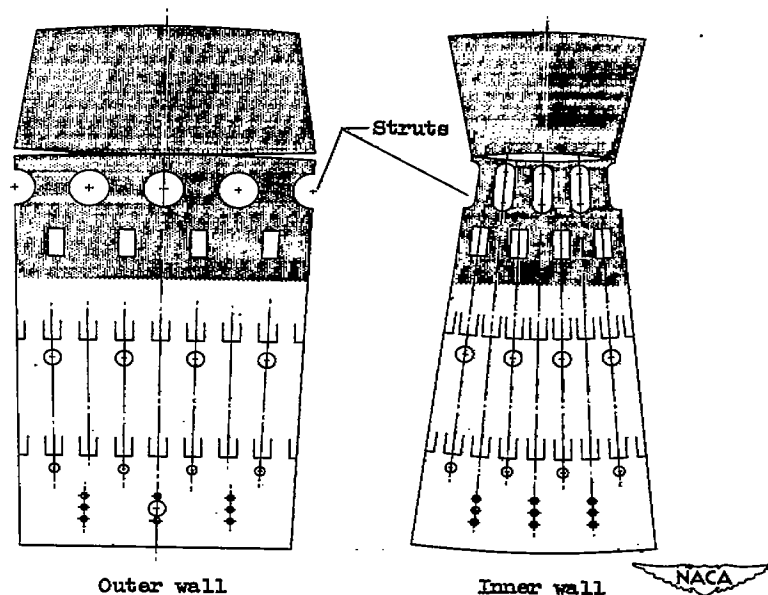
(b) Series 1-2( )$_1$; used with struts of series 1.

Figure 4. - Development of basket walls of one-sixth combustor sector.

1193

240-1625-1627

(c) Series 2-2( )$_1$ and 2-2( )$_2$; used with struts of series 1 and 2.

(d) Series 2-3( )$_2$ and 2-3C$_0$; used with struts of series 2 and without struts.
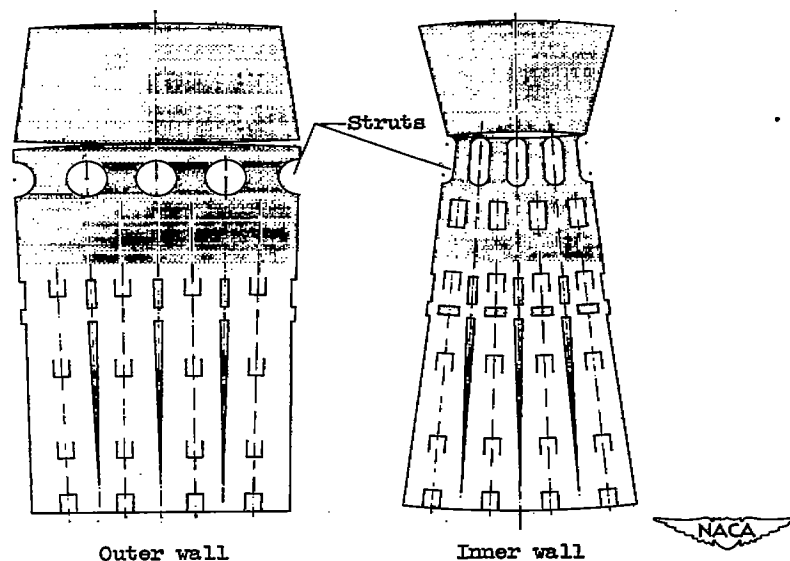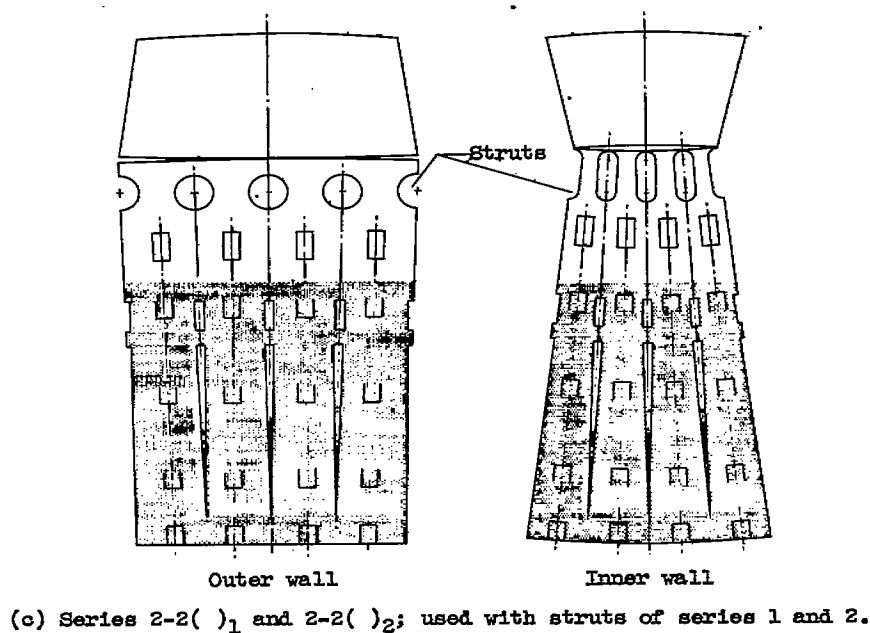
Figure 4. - Concluded. Development of basket walls of one-sixth combustor sector.

1193

Series		Primary-wall design		Secondary-wall design		Strut design	

240 +

Figure 5. - Summarization of basket modifications.
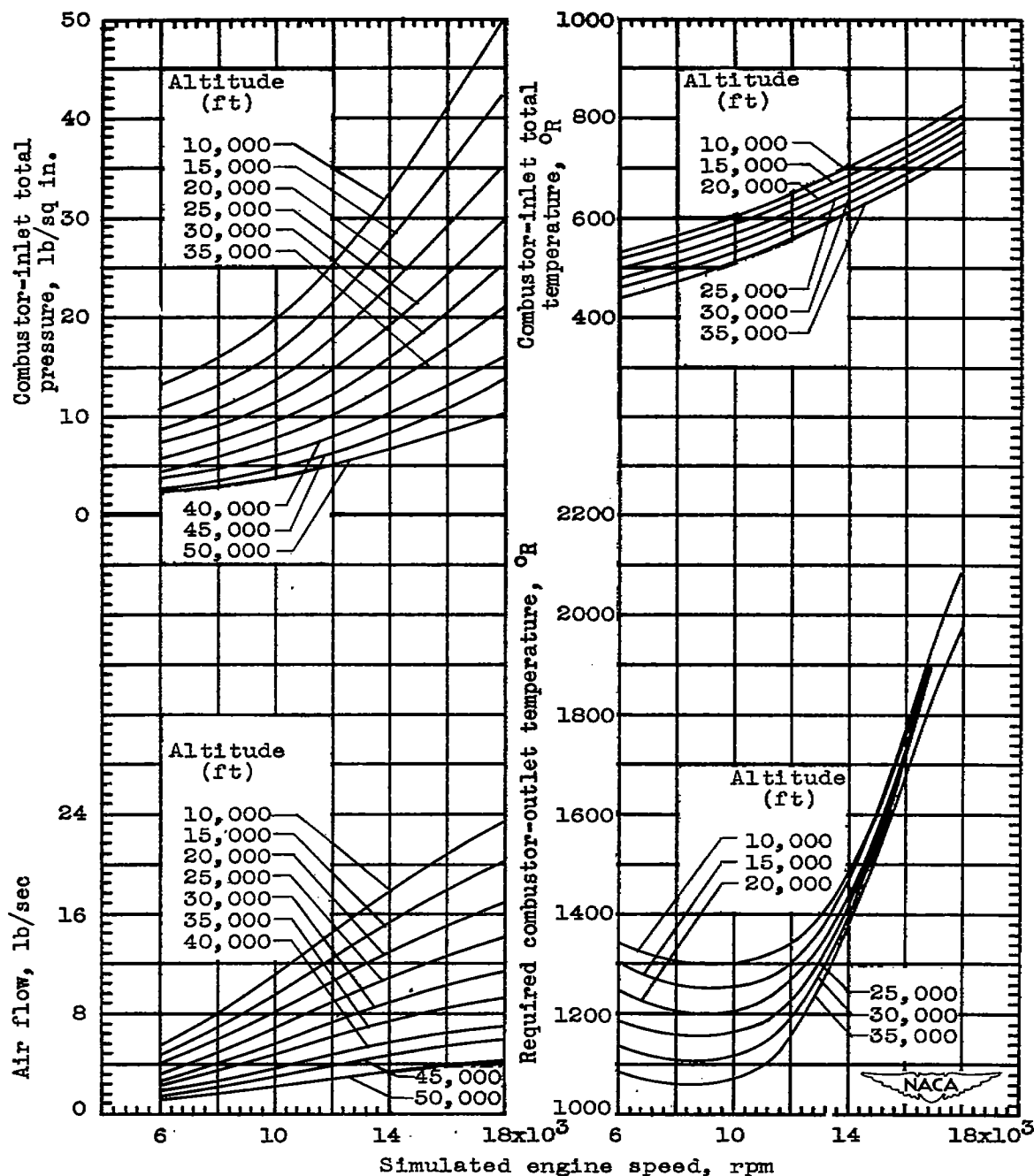
Figure 6. - Operating characteristics of a contemporary annular turbojet engine at flight speed of 0 mile per hour. (Estimated data obtained from reference 1.)
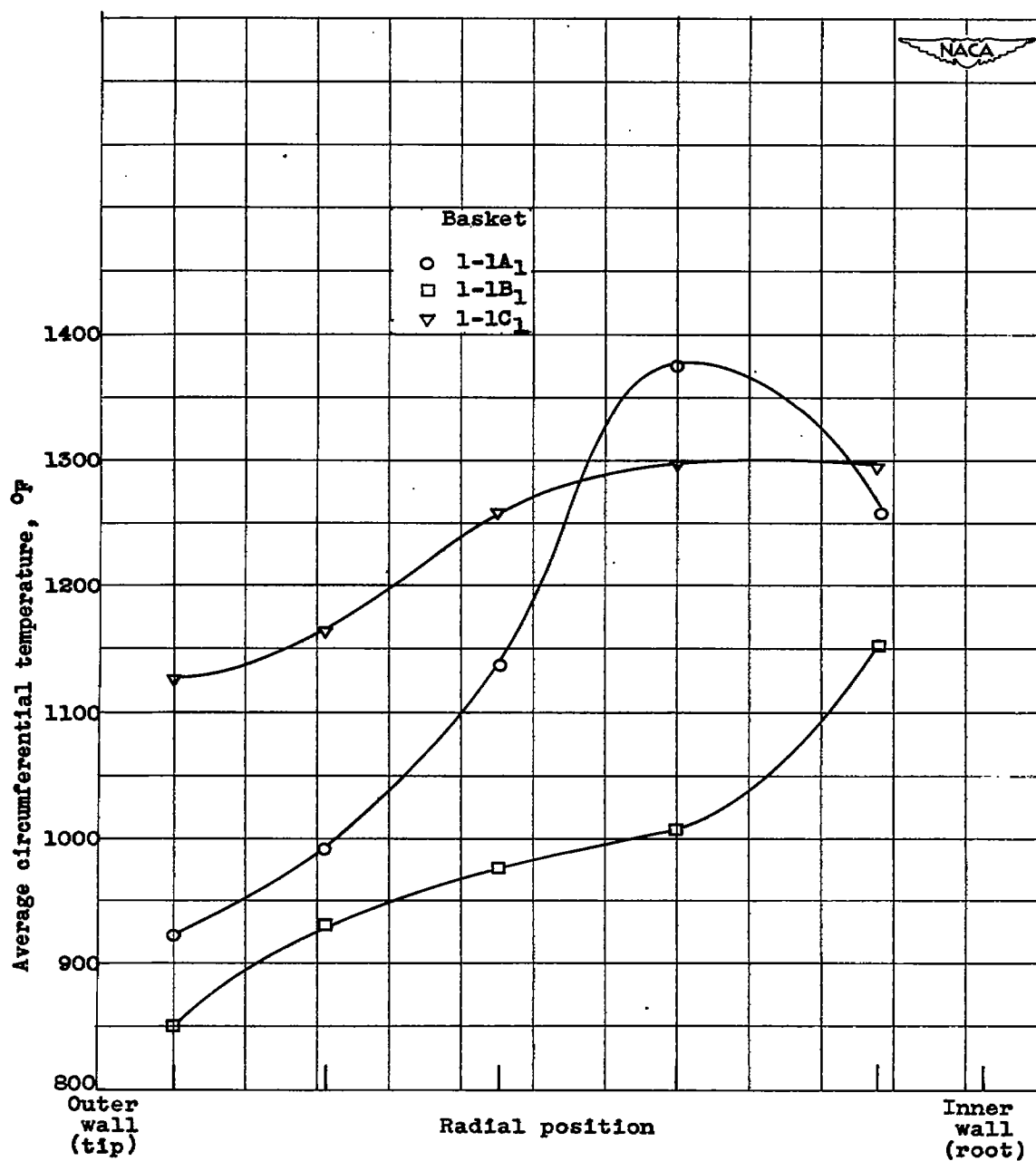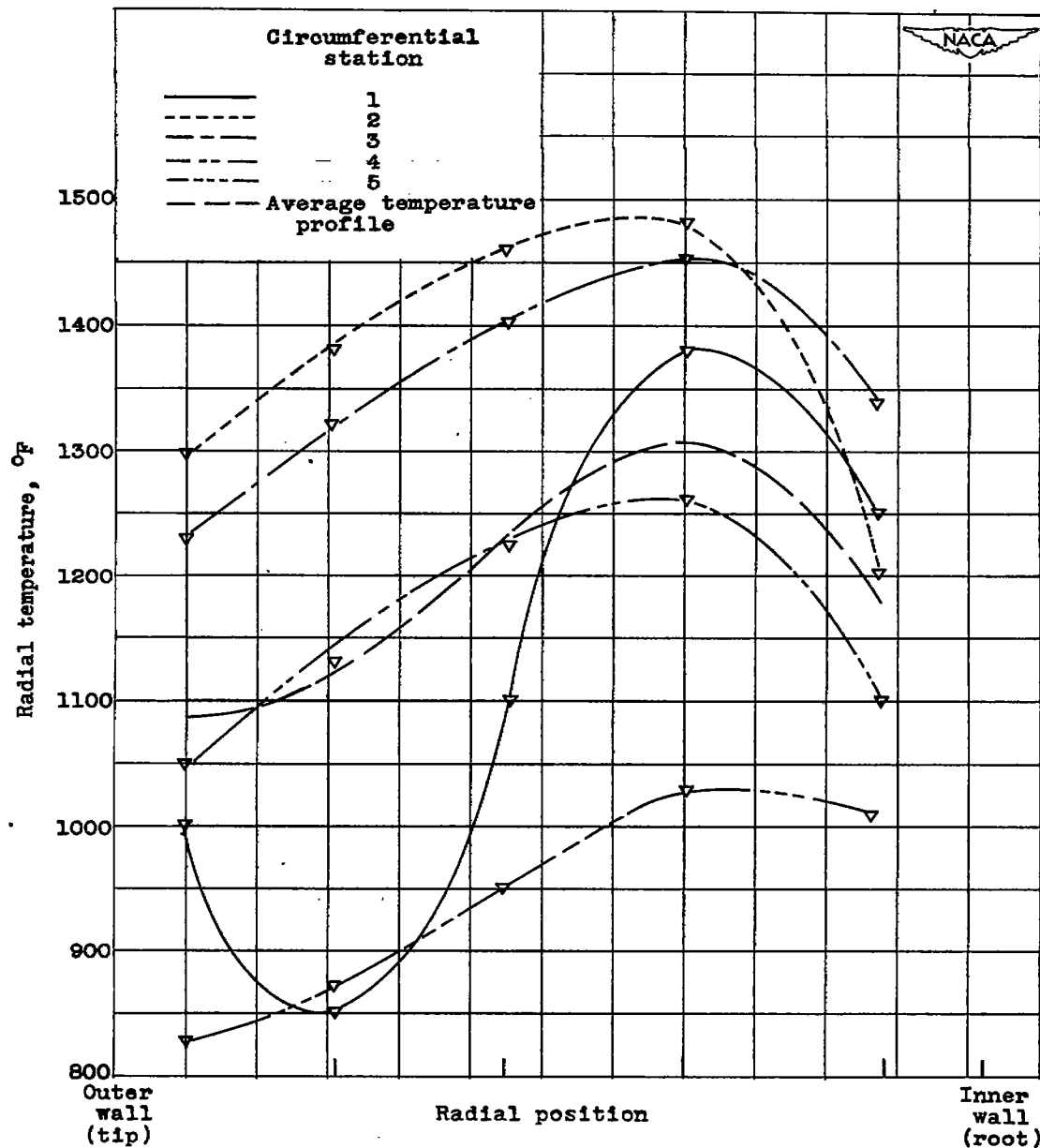
(a) Radial temperature distribution. Operating conditions:
       altitude, 40,000 feet; engine speed, 17,400 rpm; fuel-air
       ratio, 0.016.

Figure 7. – Performance characteristics of one-sixth sector of annular
           turbojet combustor in series 1-1( )$_1$.
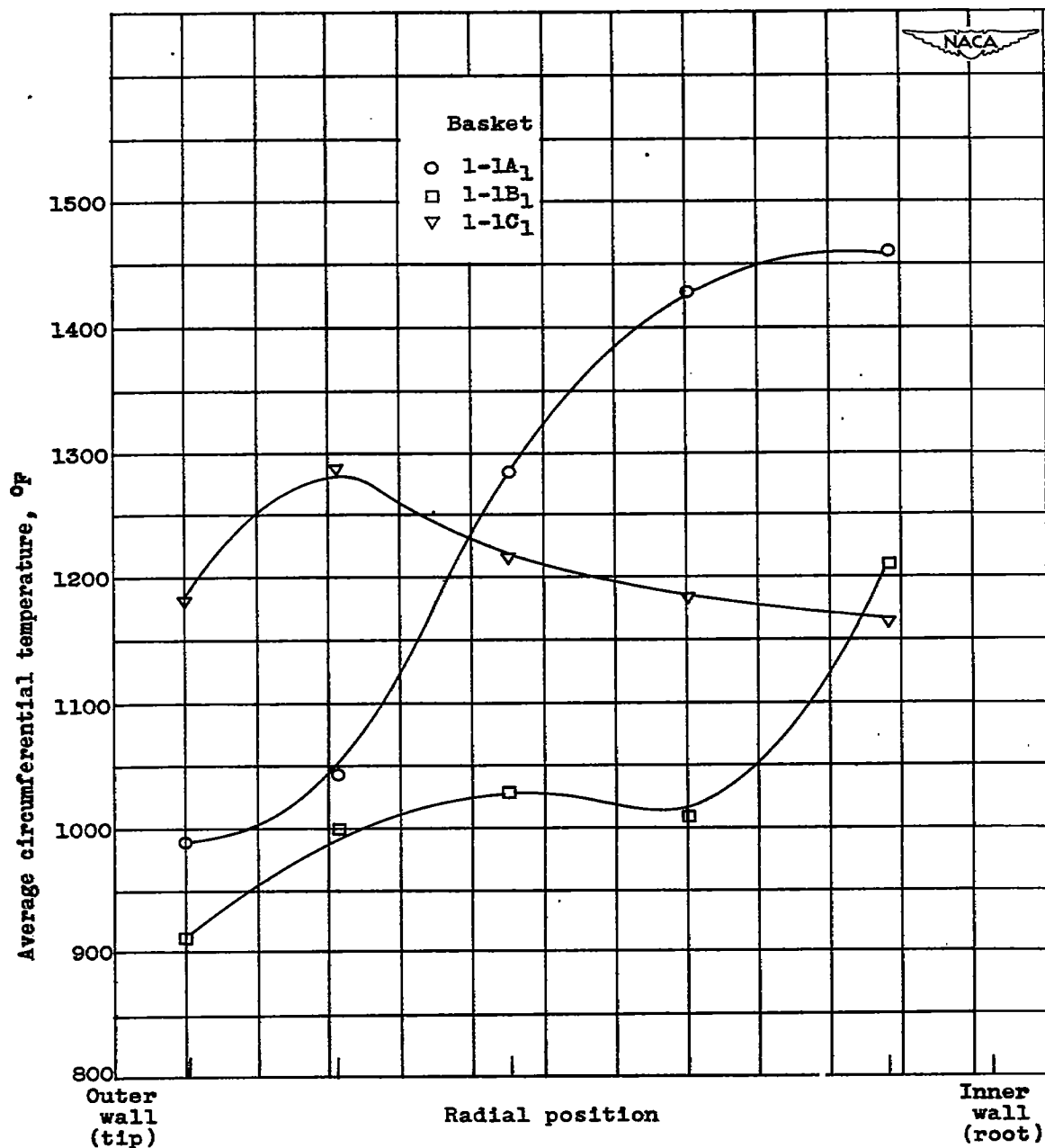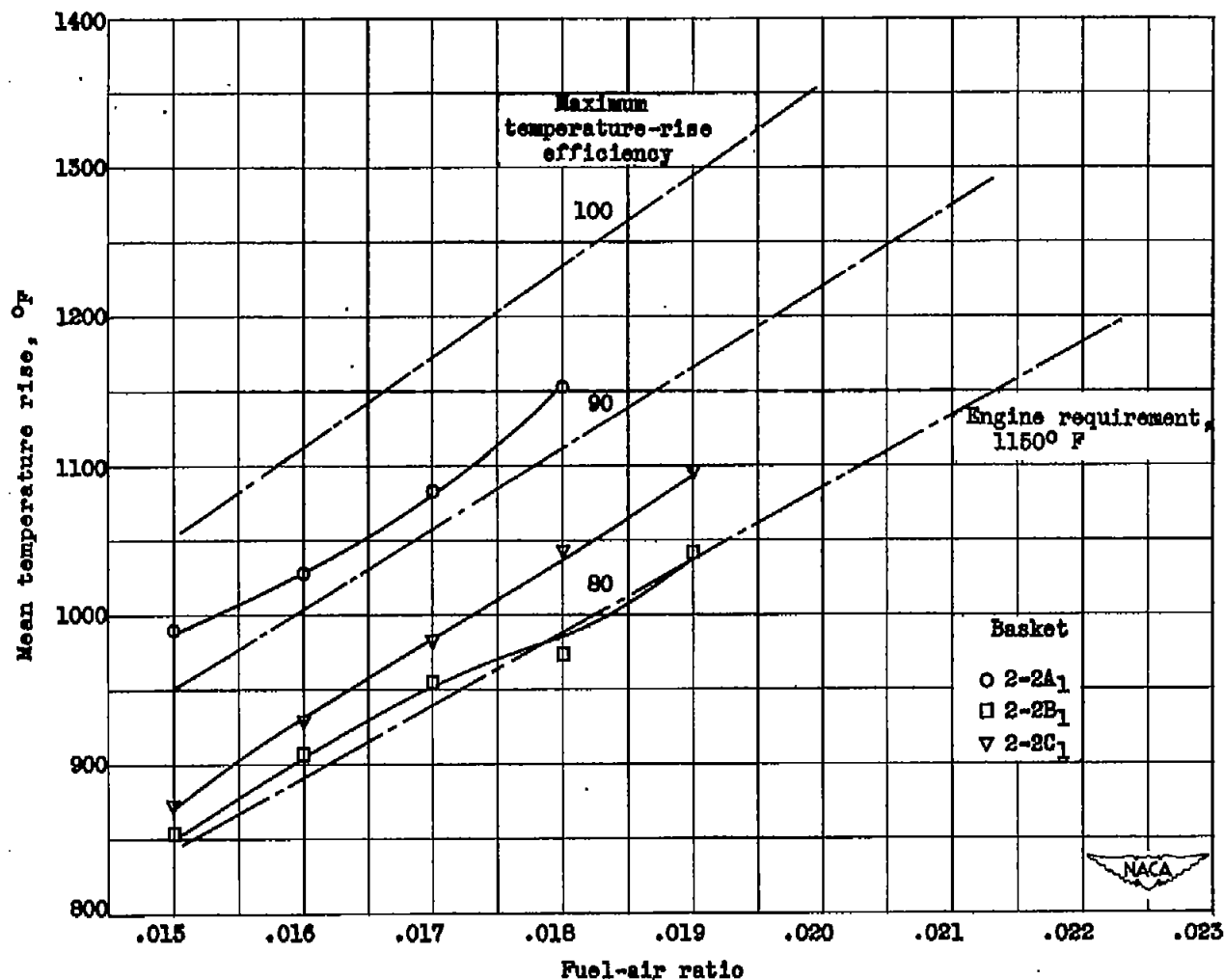
(b)   Radial temperature distribution.   Operating conditions:
          altitude, 30,000 feet; engine speed, 17,400 rpm; fuel-air
          ratio, 0.016.

Figure 7. - Continued.   Performance characteristics of one-sixth sector
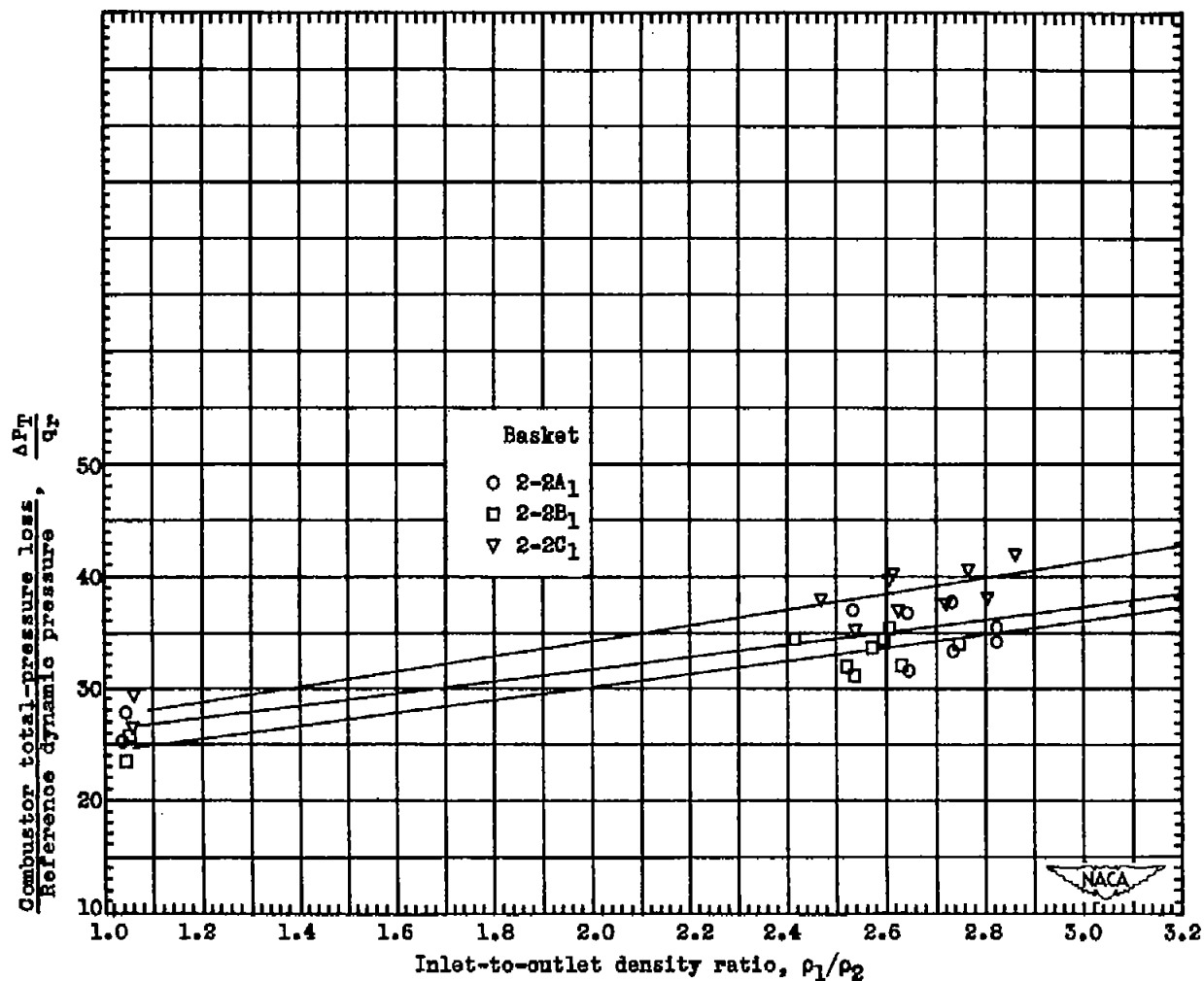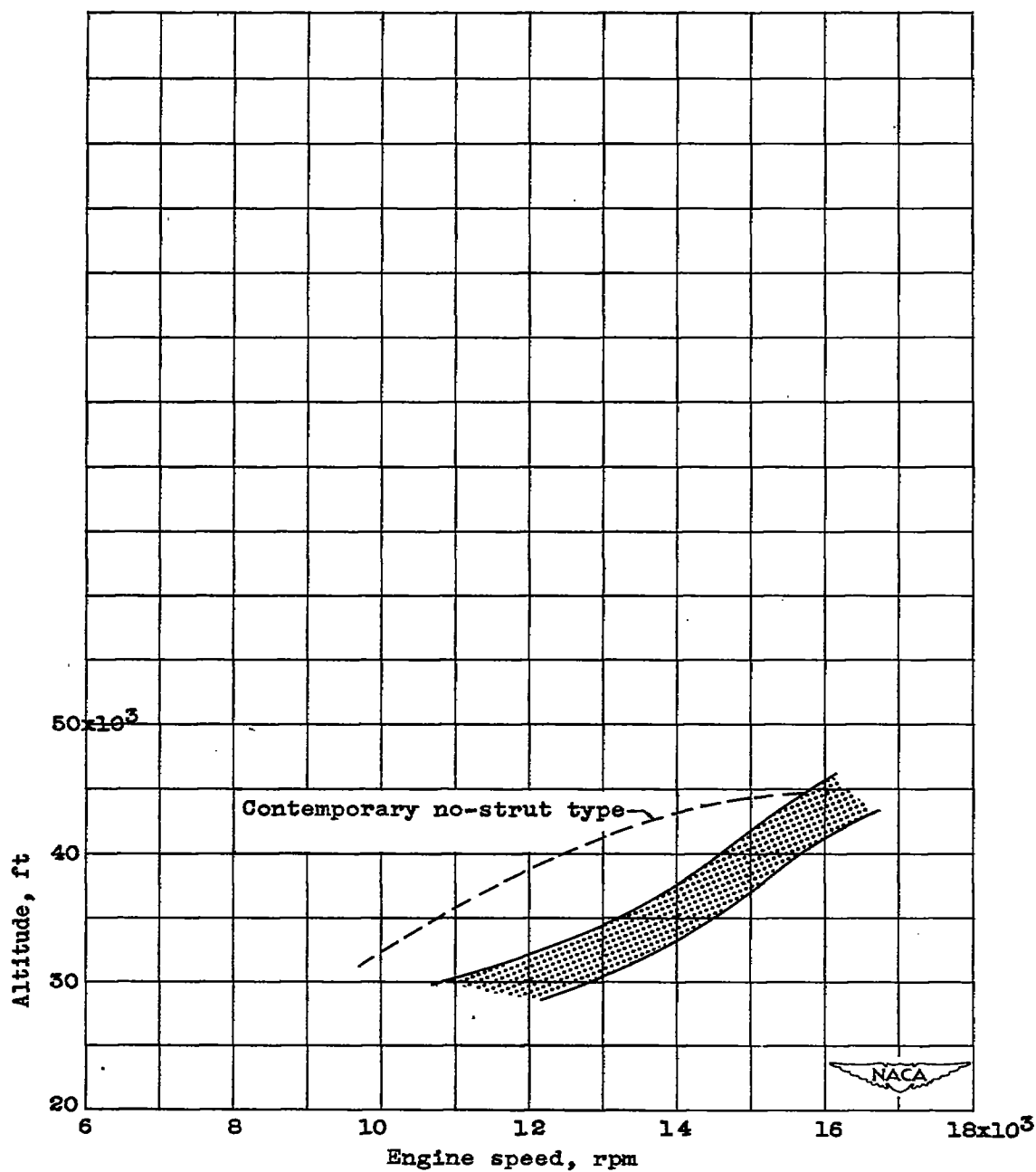   of annular turbojet combustor in series 1-1( )₁.
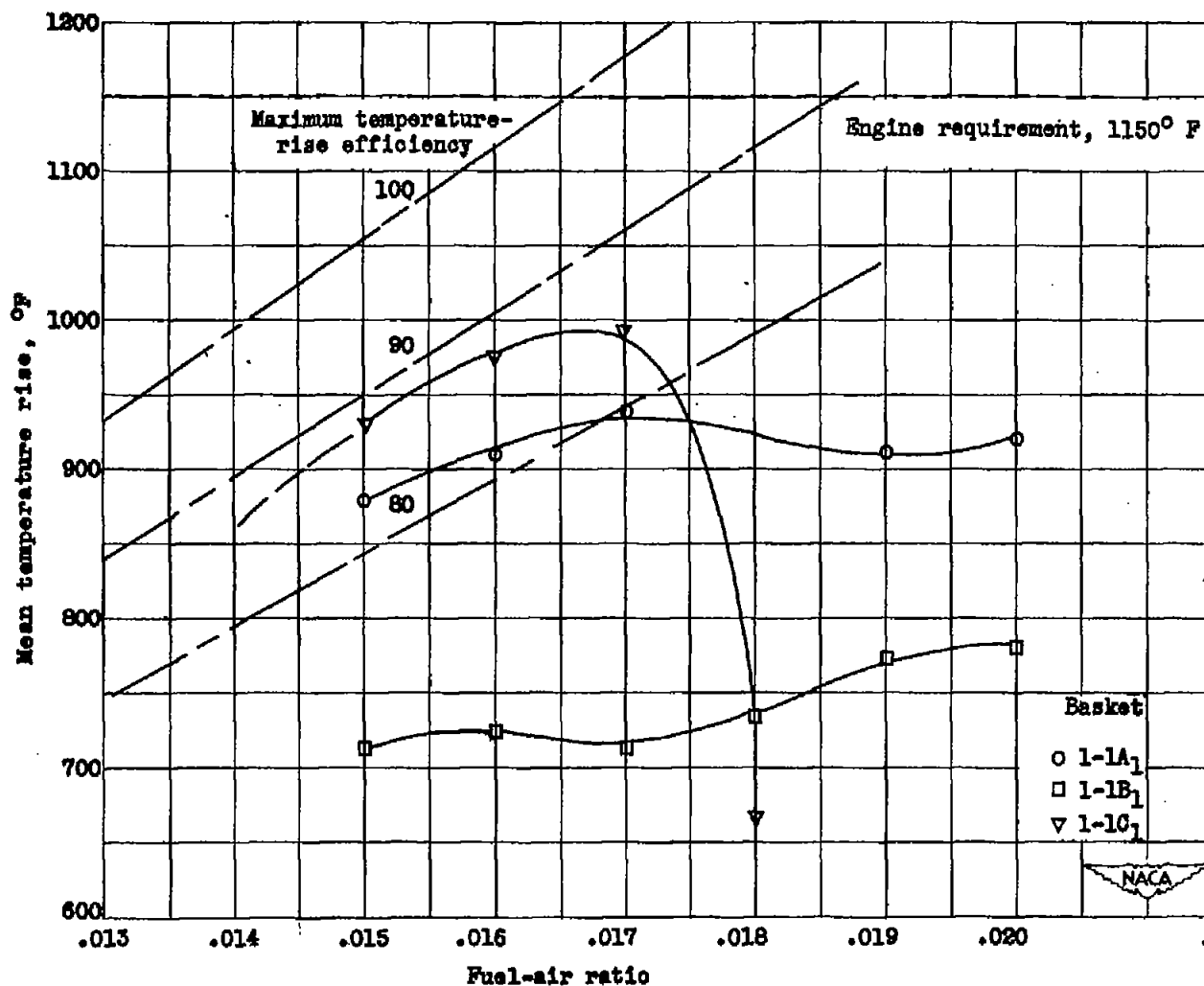
(c) Variation of mean temperature rise with fuel-air ratio. Operating conditions:
altitude, 40,000 feet; engine speed, 17,400 rpm.

Figure 7. - Continued. Performance characteristics of one-sixth sector of annular turbojet
combustor in series 1-1( )$_1$.
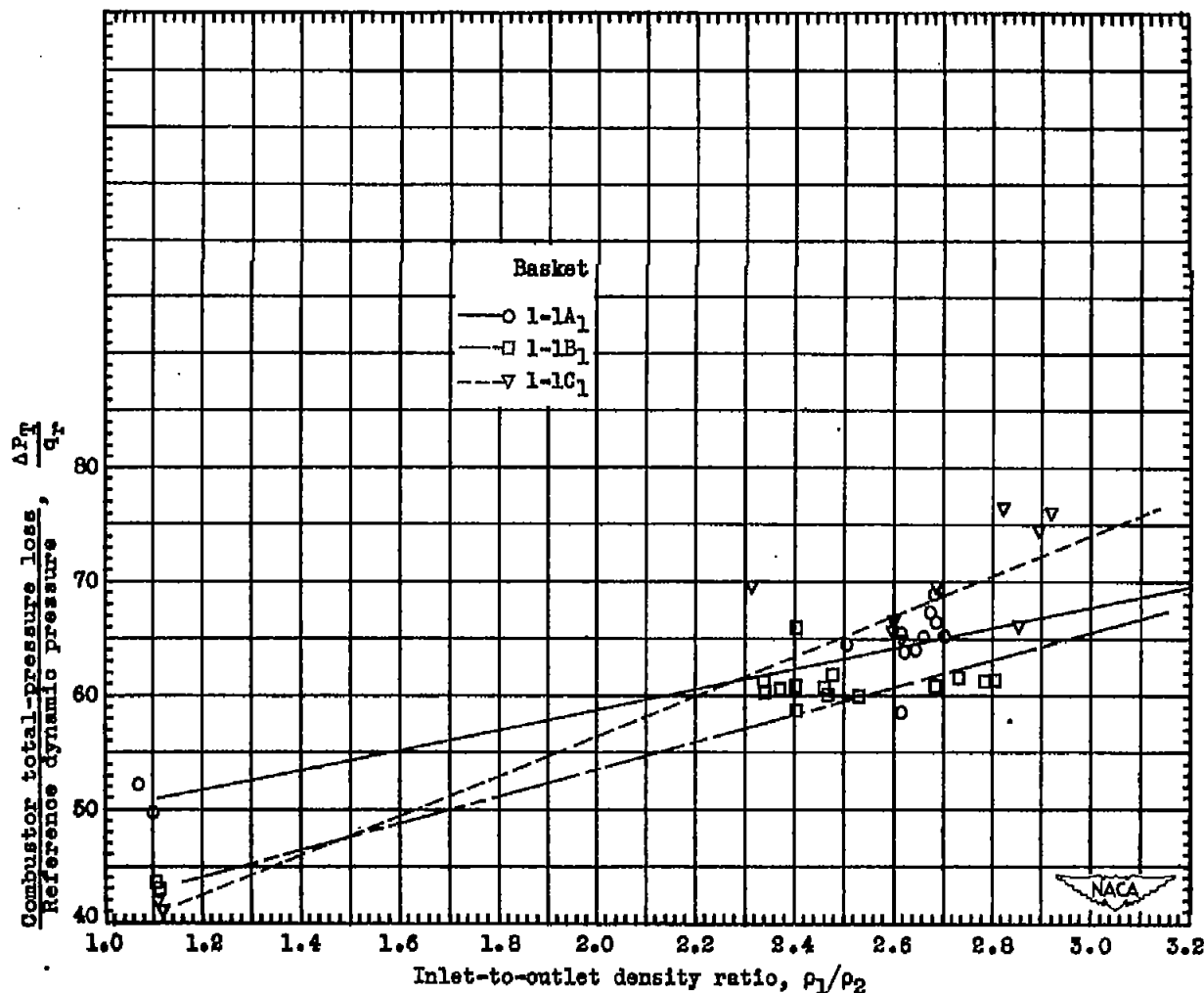
(d) Total-pressure loss shown as a function of inlet-to-outlet density ratio. Operating conditions: altitude, 40,000 feet; engine speed, 17,400 rpm.

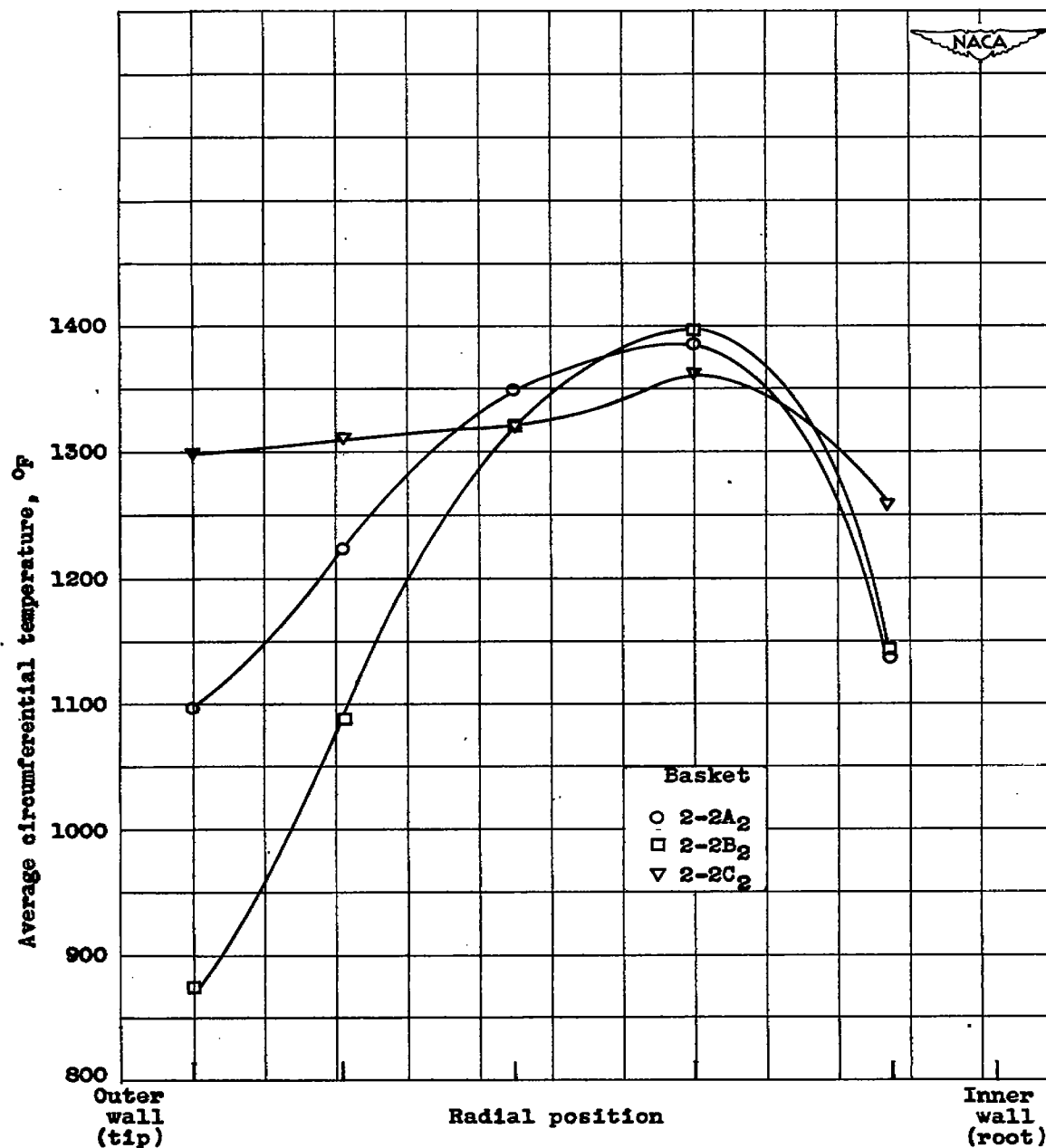Figure 7. - Continued. Performance characteristics of one-sixth sector of annular turbojet combustor in series 1-1( )$_1$.

1193
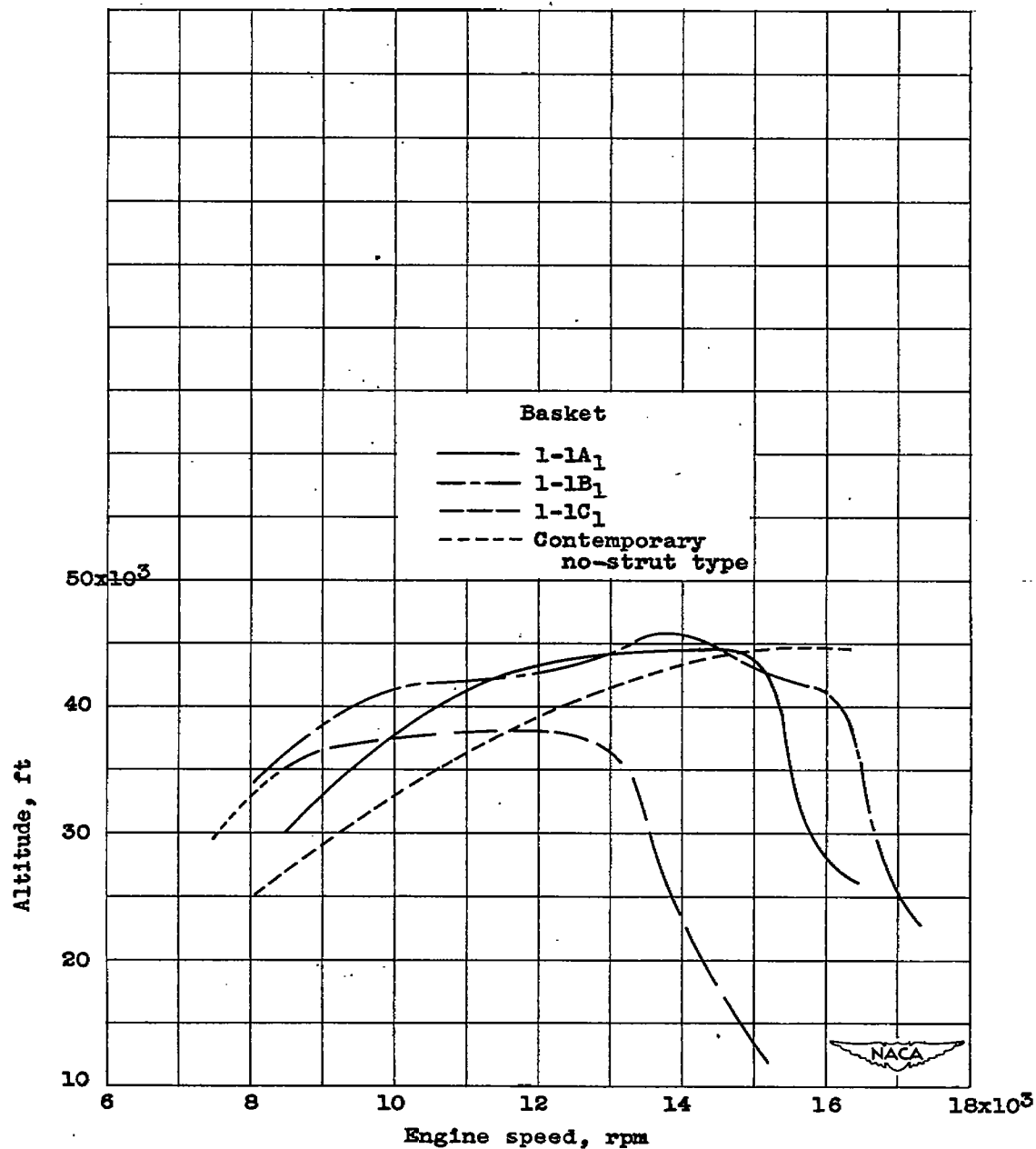
(e) Altitude operating limits.

Figure 7. - Concluded. Performance characteristics of one-sixth sector
of annular turbojet combustor in series 1-1( )$_1$.

1193
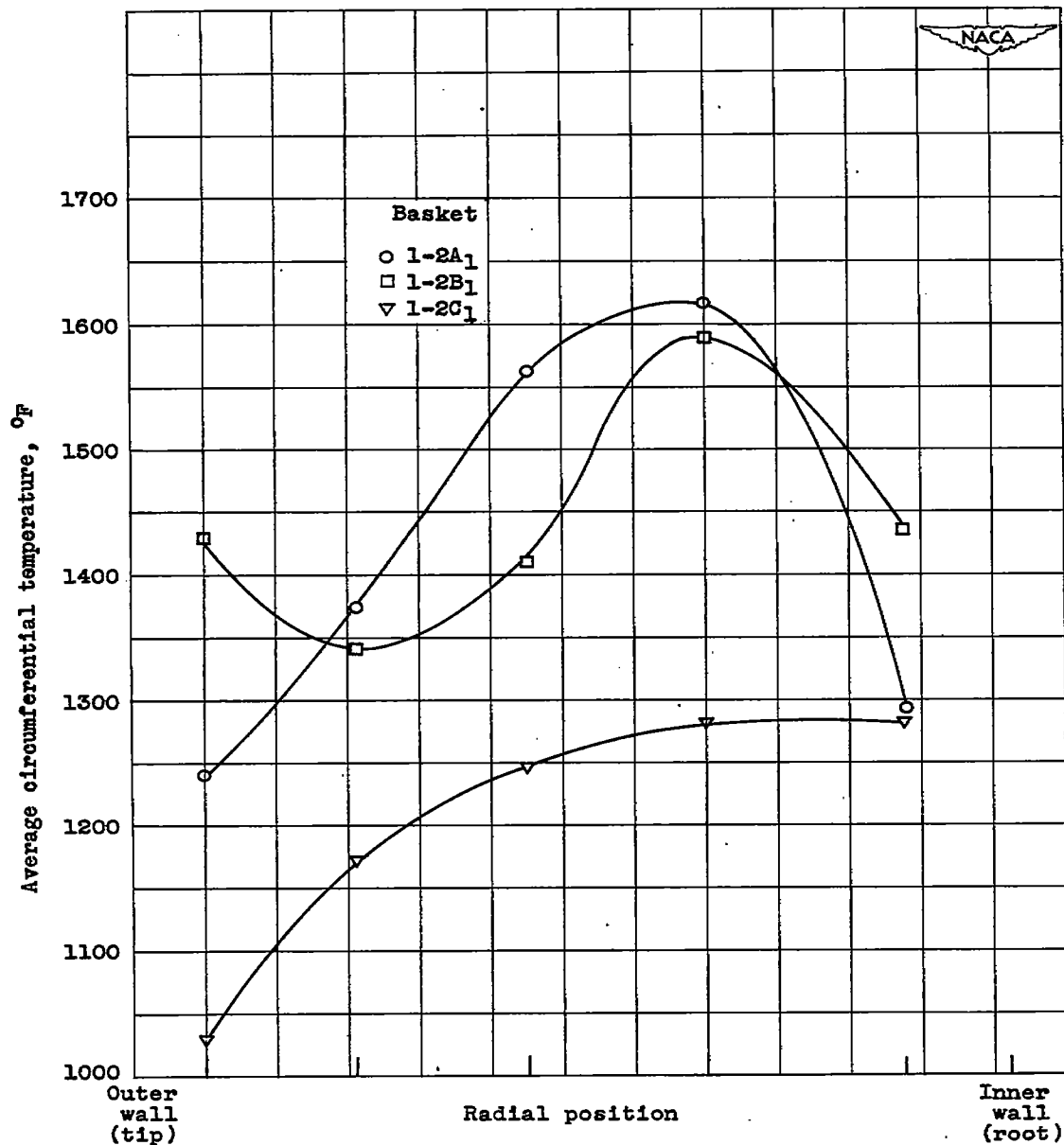
(a) Radial temperature distribution. Operating conditions:
altitude, 40,000 feet; engine speed, 17,400 rpm; fuel-air
ratio, 0.016.

Figure 8. - Performance characteristics of one-sixth sector of annular turbo-
jet combustor in series 1-2( )$_1$.

1193
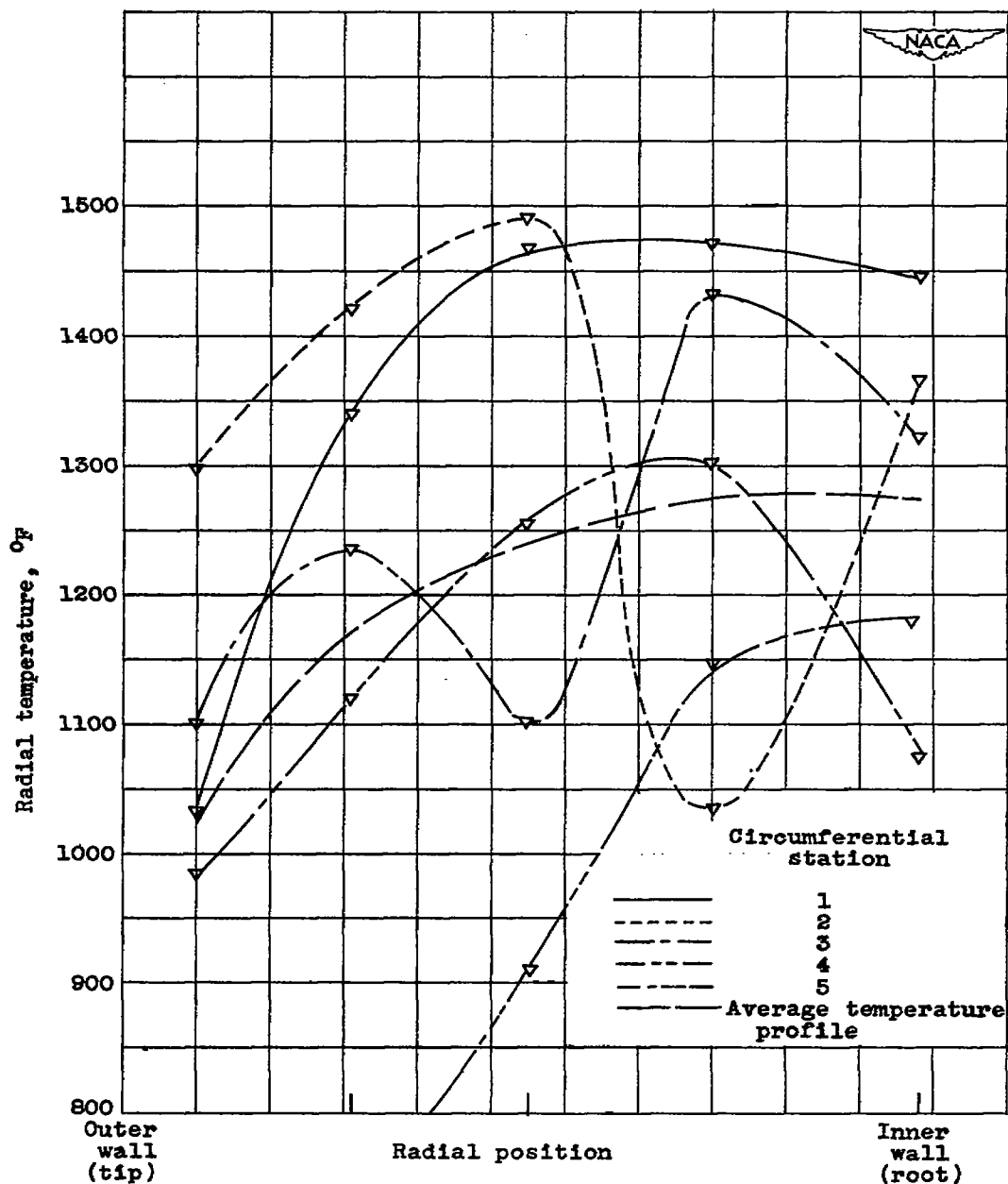
(b) Radial temperature distribution at five circumferential
     stations. Basket 1-2C$_1$; operating conditions: altitude,
     40,000 feet; engine speed, 17,400 rpm; fuel-air ratio,
     0.016.

Figure 8. - Continued. Performance characteristics of one-sixth sector
     of annular turbojet combustor in series 1-2( )$_1$.
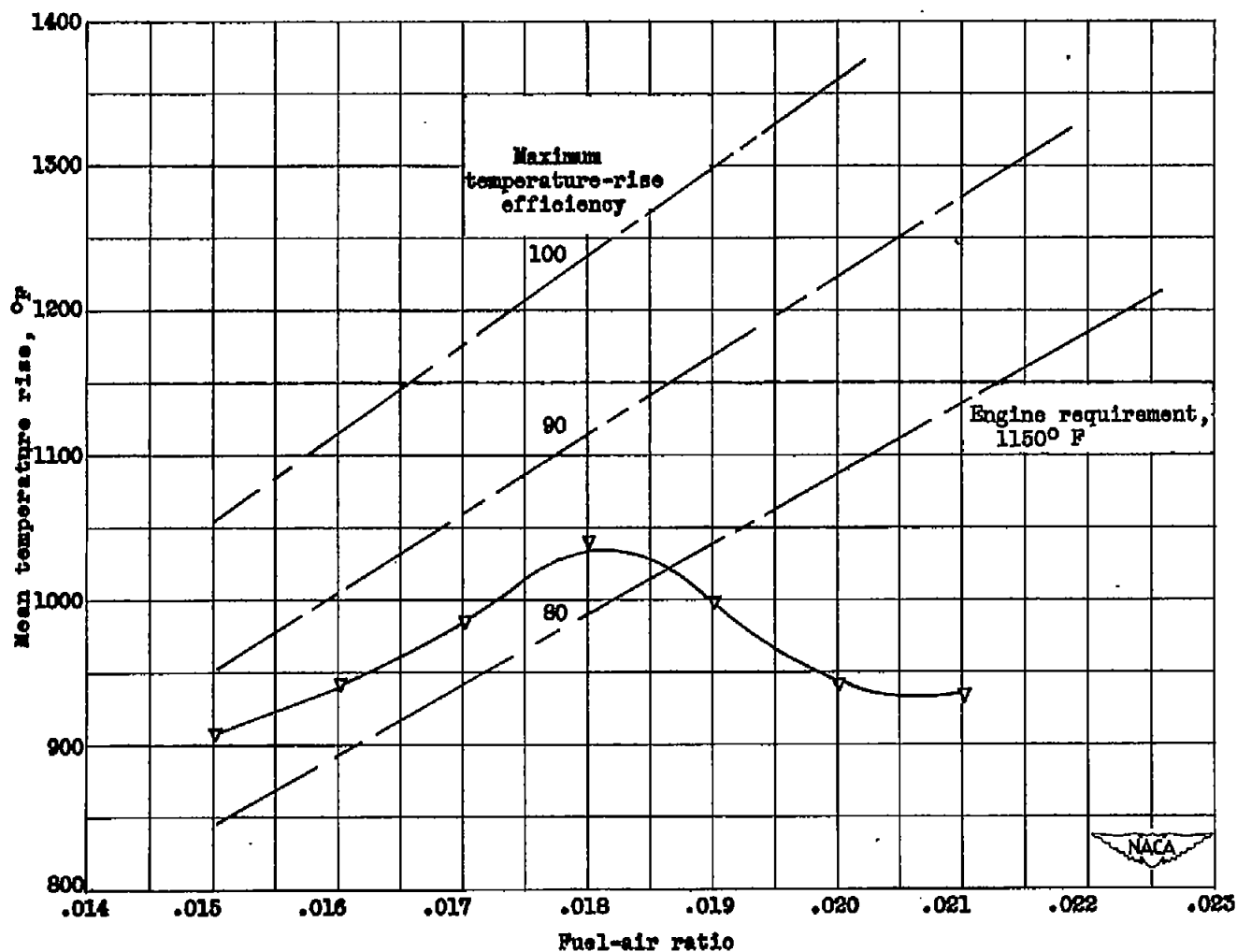
(c)   Variation of mean temperature rise with fuel-air ratio. Basket 1-2C$_1$; operating
conditions: altitude, 40,000 feet; engine speed, 17,400 rpm.

Figure 8. - Continued. Performance characteristics of one-sixth sector of annular turbojet combustor
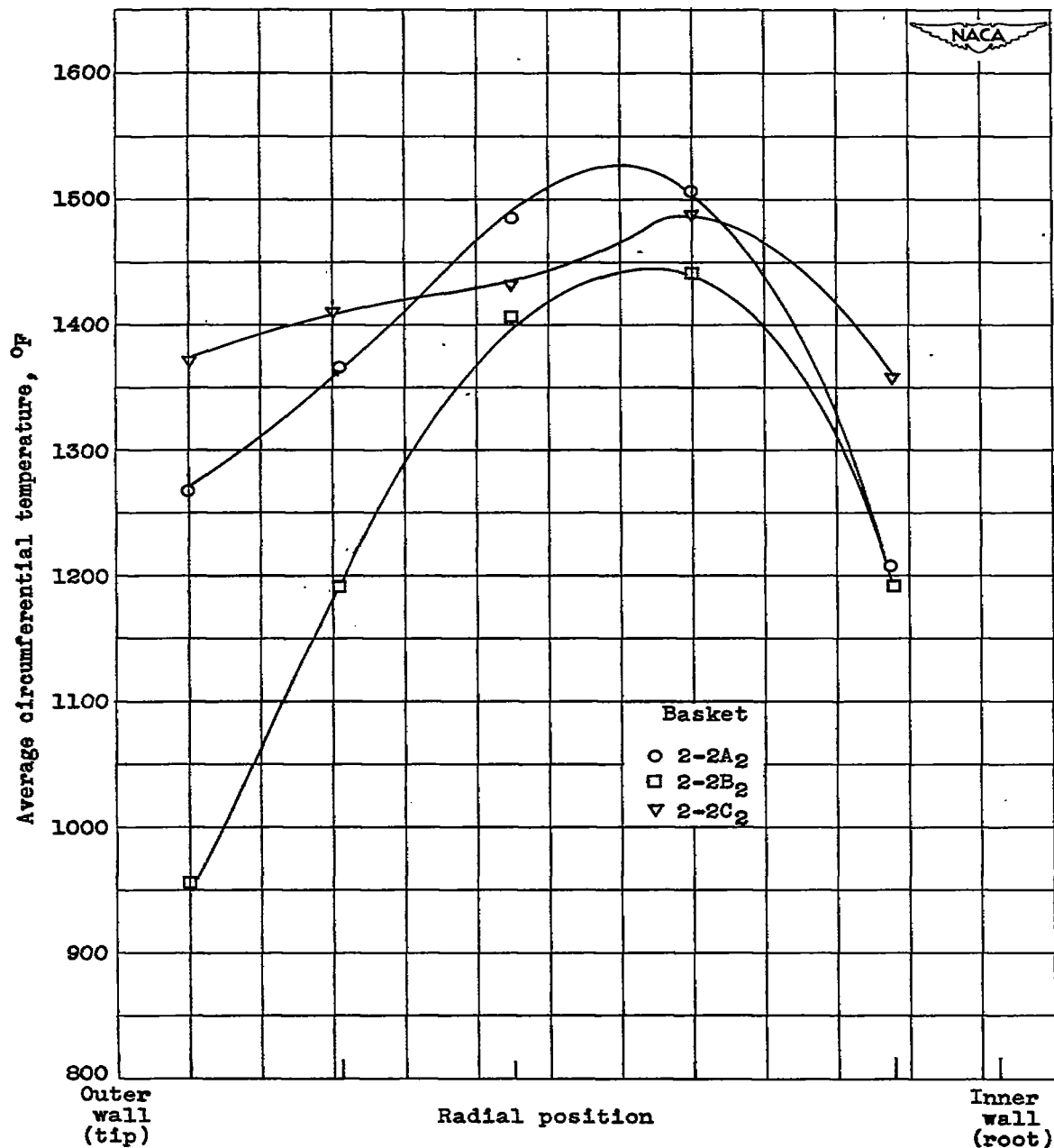in series 1-2( )$_1$.
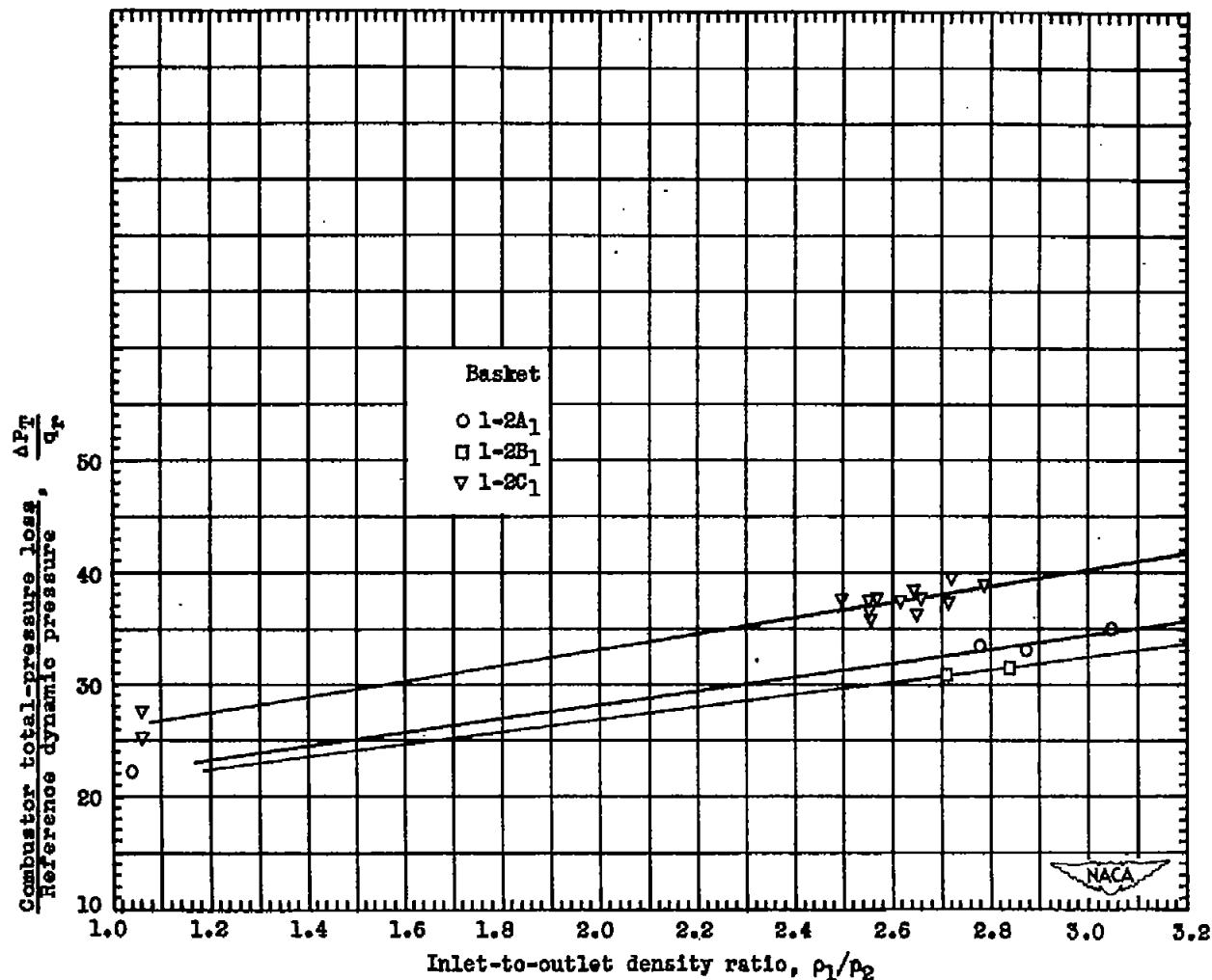
(d) Total-pressure loss shown as function of inlet-to-outlet density ratio. Operating
conditions: altitude, 40,000 feet; engine speed, 17,400 rpm.

Figure 8. - Continued. Performance characteristics of one-sixth sector of annular turbojet
combustor in series 1-2( )$_1$.
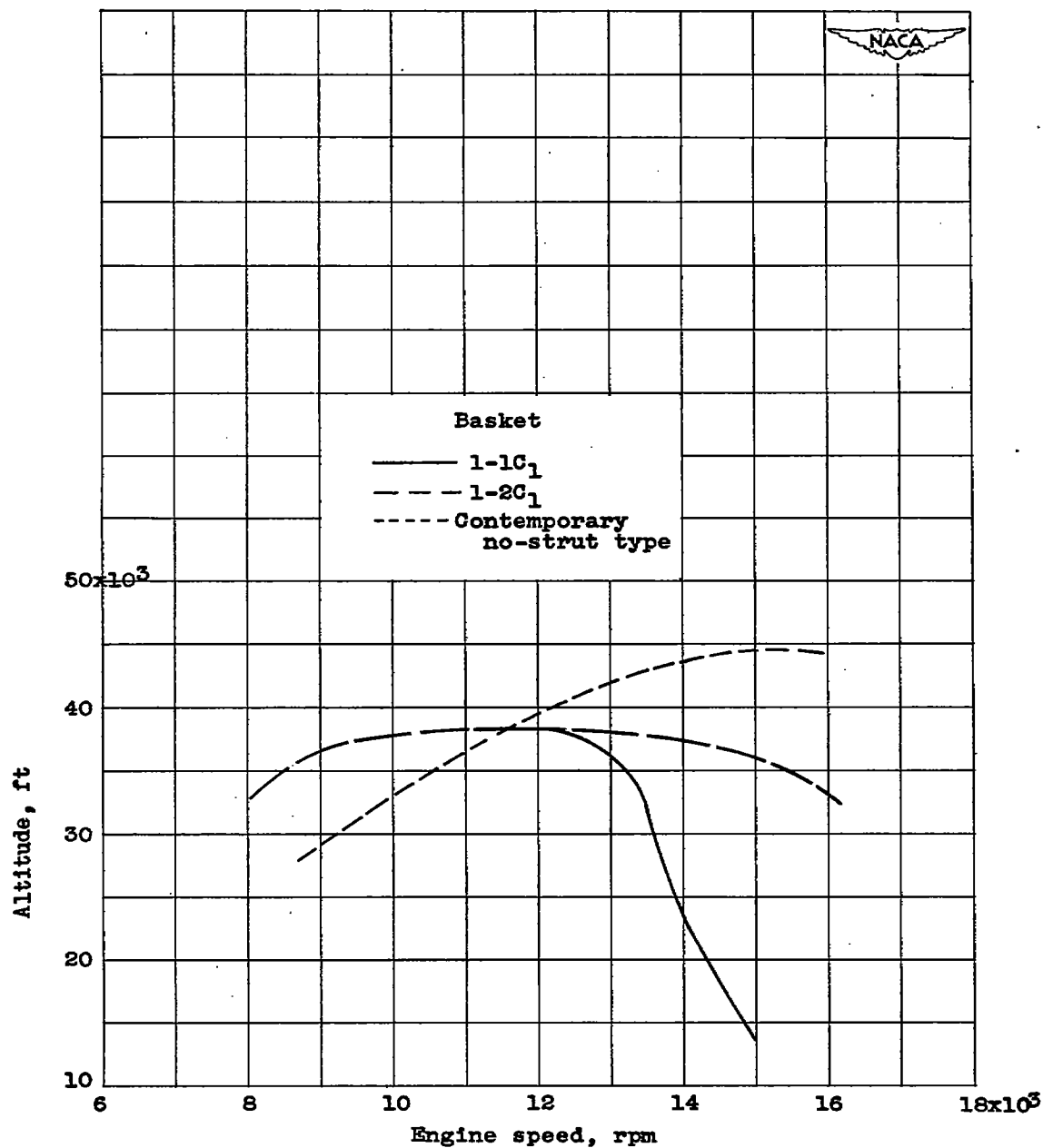
(e) Altitude operating limits.

Figure 8. - Concluded. Performance characteristics of one-sixth sector
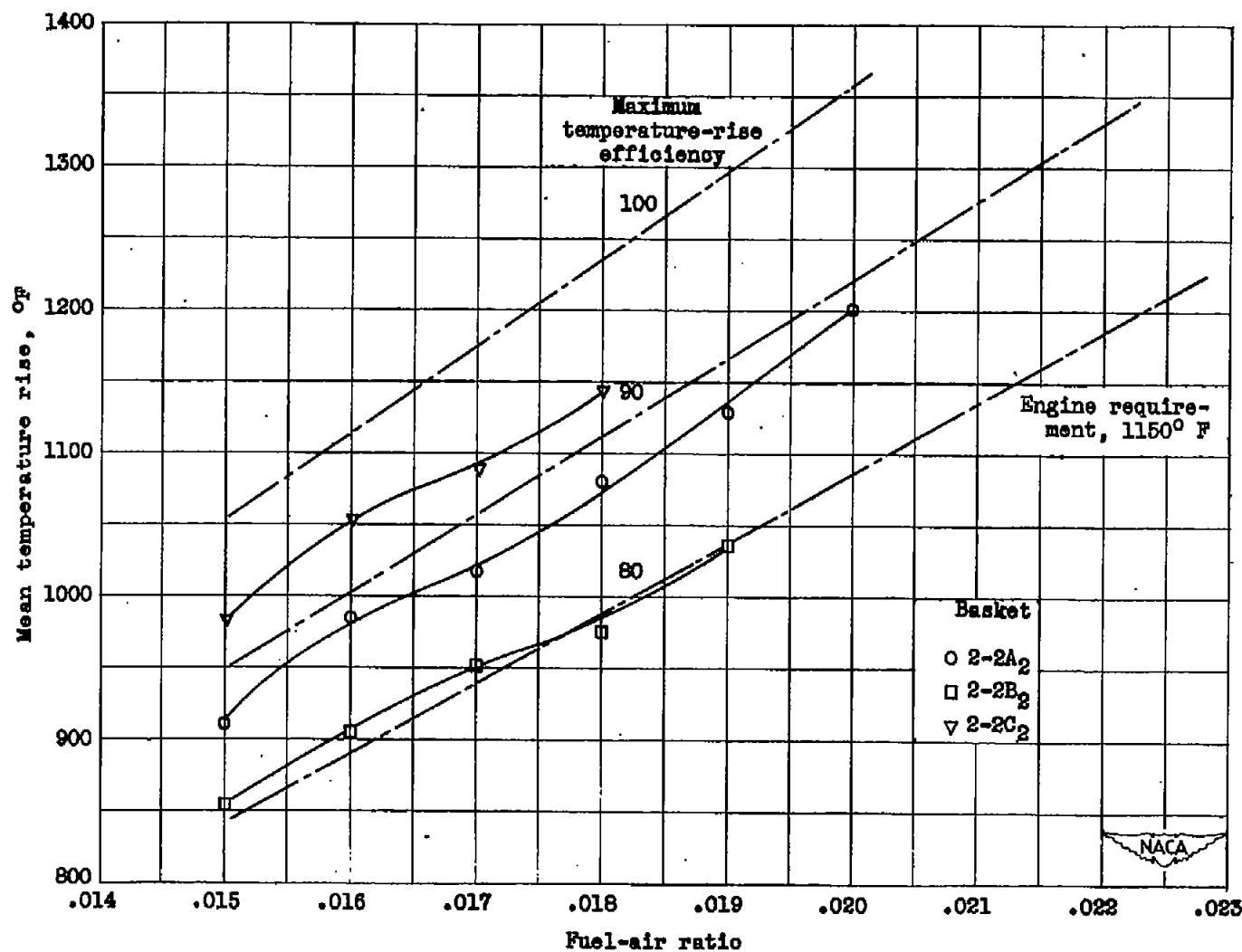of annular turbojet combustor in series 1-2( )$_1$.
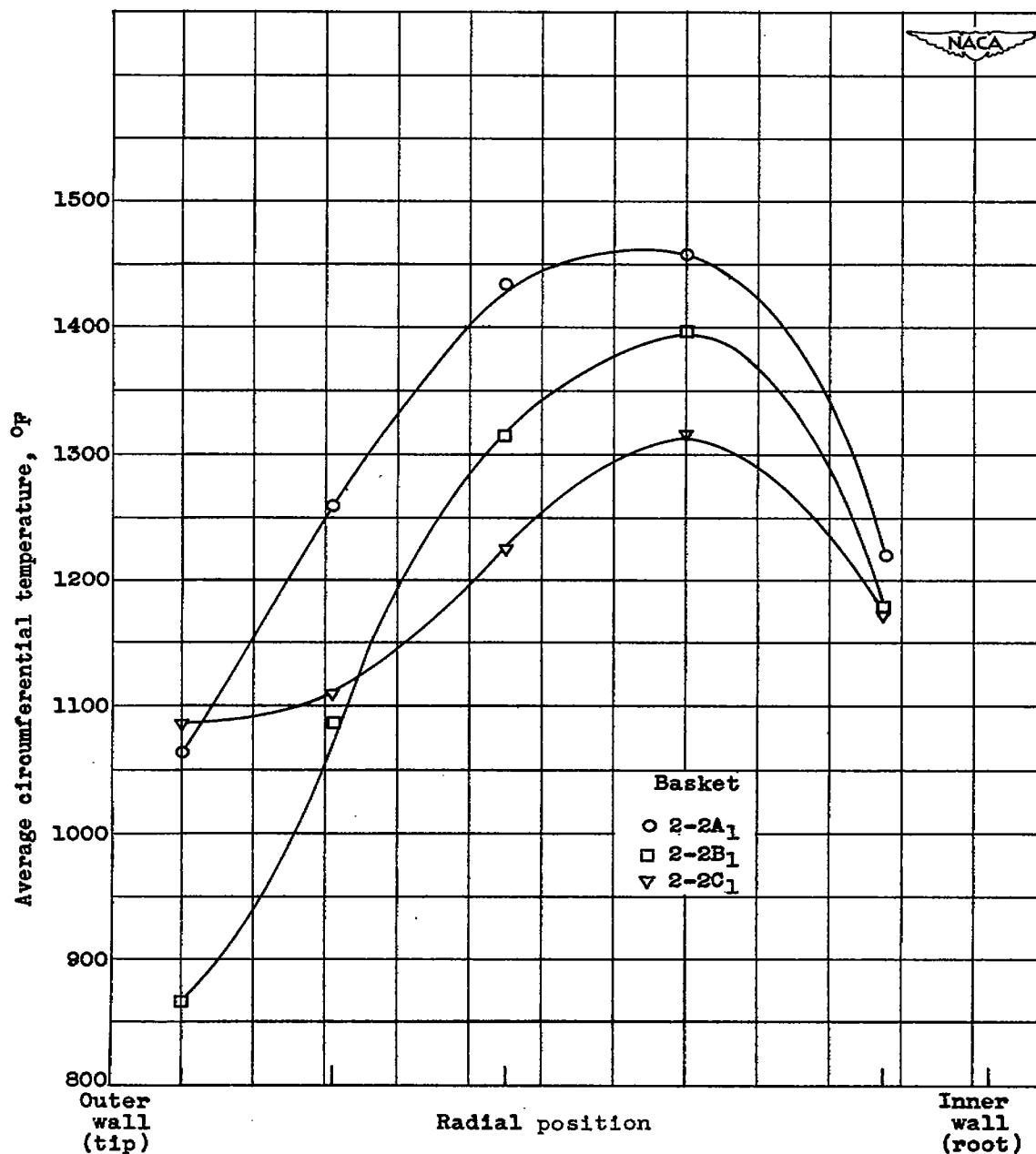
(a) Radial temperature distribution. Operating conditions: altitude, 40,000 feet; engine speed, 17,400 rpm; fuel-air ratio, 0.016.

Figure 9. - Performance characteristics of one-sixth sector of annular turbojet combustor in series 2-2( )$_1$.
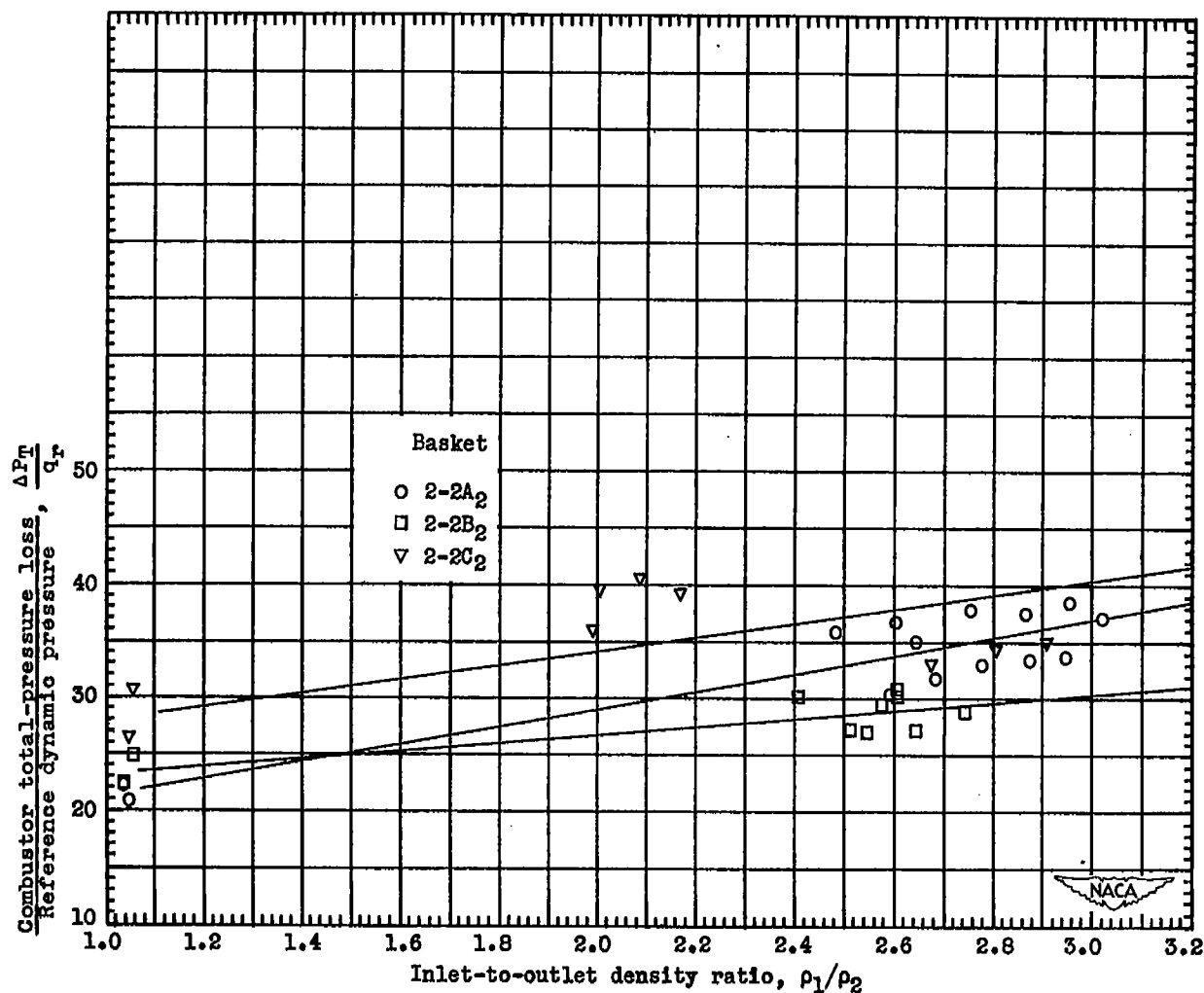
1193

(b) Radial temperature distribution. Operating conditions:
       altitude, 30,000 feet; engine speed, 17,400 rpm; fuel-air
       ratio, 0.016.

Figure 9. - Continued. Performance characteristics of one-sixth sector
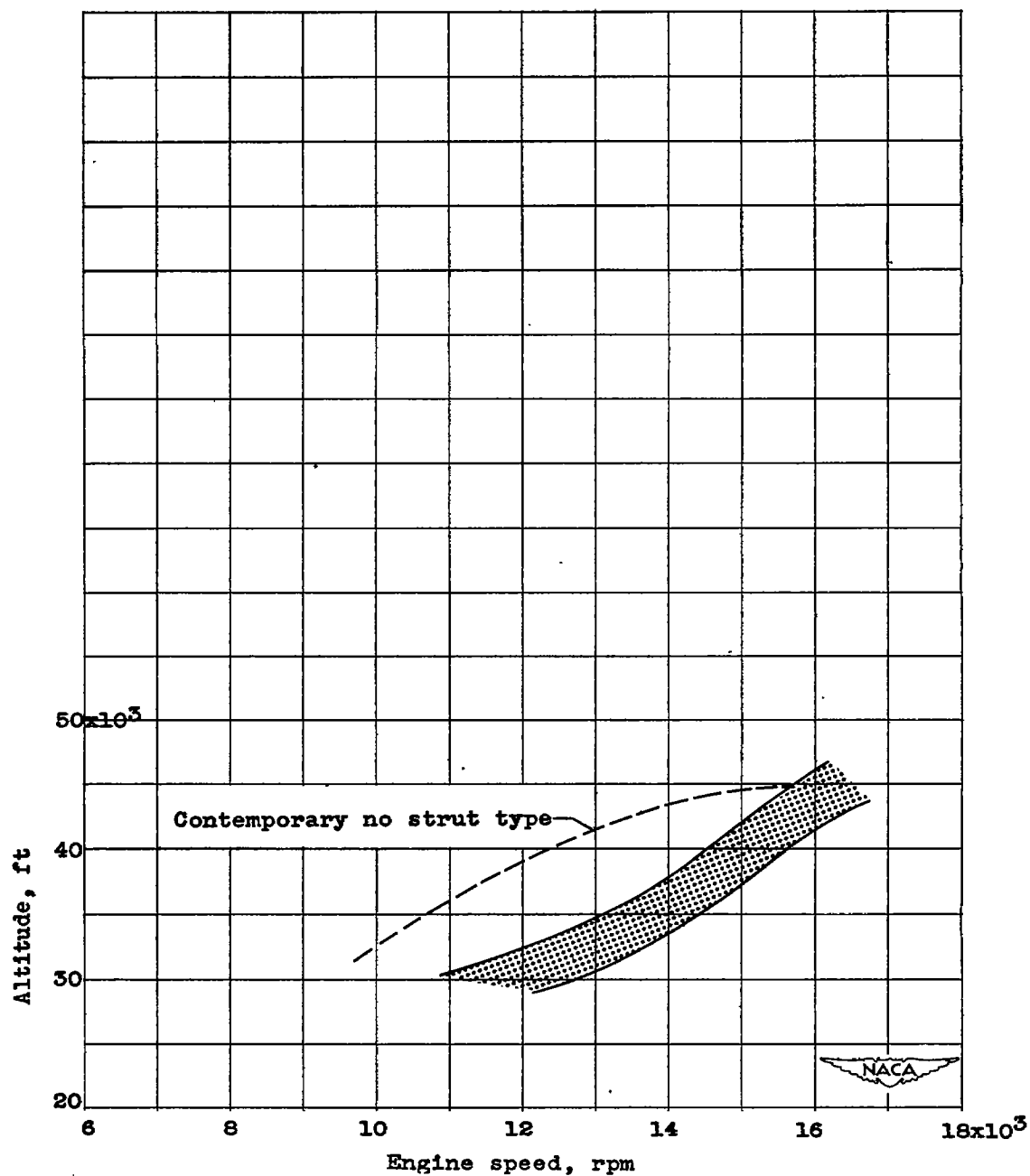   of annular turbojet combustor in series 2-2( )$_1$.

1193
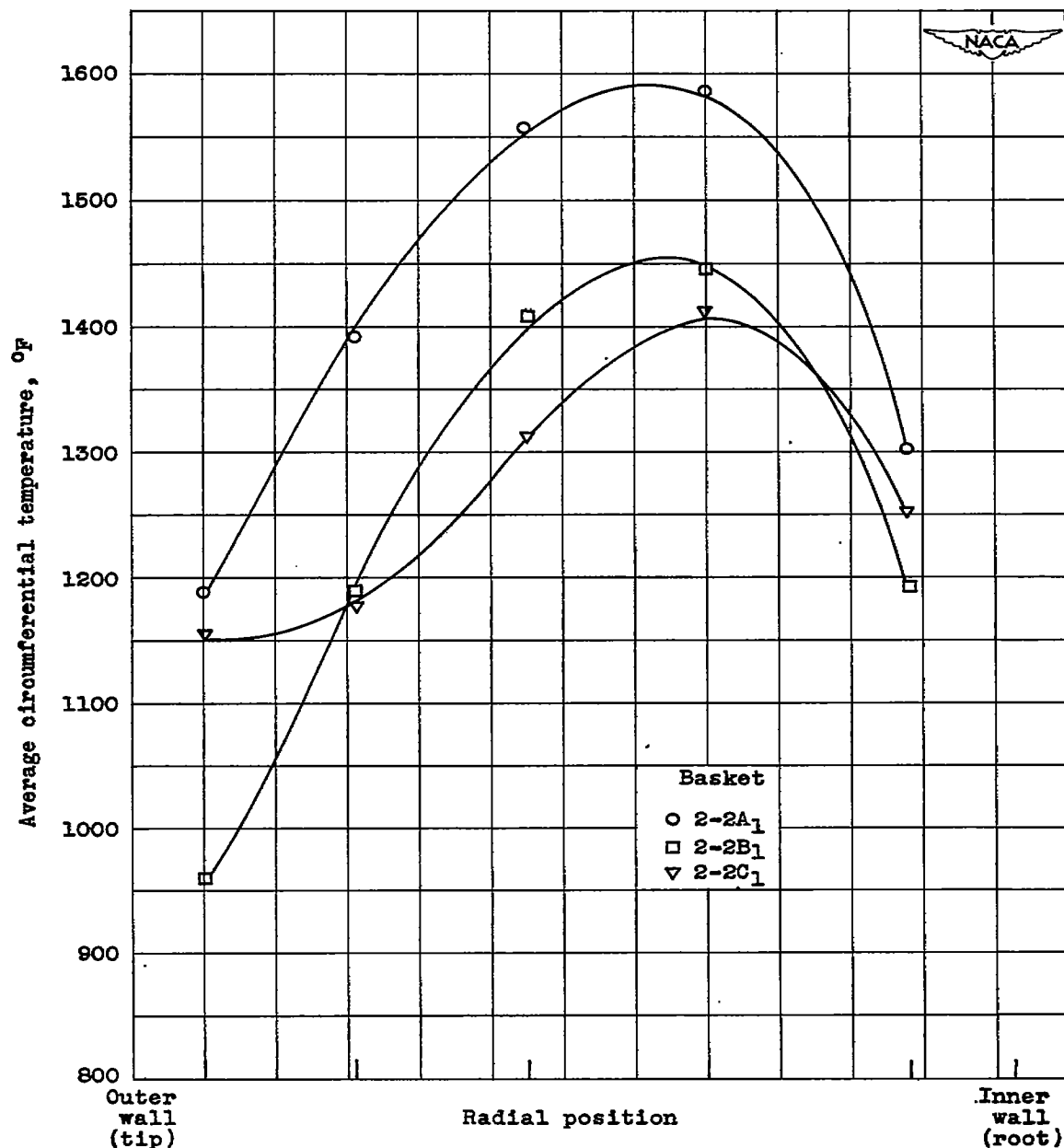
(c) Radial temperature distribution at five circumferential stations.
     Basket 2-2C$_1$; operating conditions: altitude, 40,000 feet;
     engine speed, 17,400 rpm; fuel-air ratio, 0.016.

Figure 9. - Continued. Performance characteristics of one-sixth sector
     of annular turbojet combustor in series 2-2( )$_1$.

(d) Variation of mean temperature rise with fuel-air ratio. Operating conditions:
altitude, 40,000 feet; engine speed, 17,400 rpm.

Figure 9. - Continued. Performance characteristics of one-sixth sector of annular turbojet
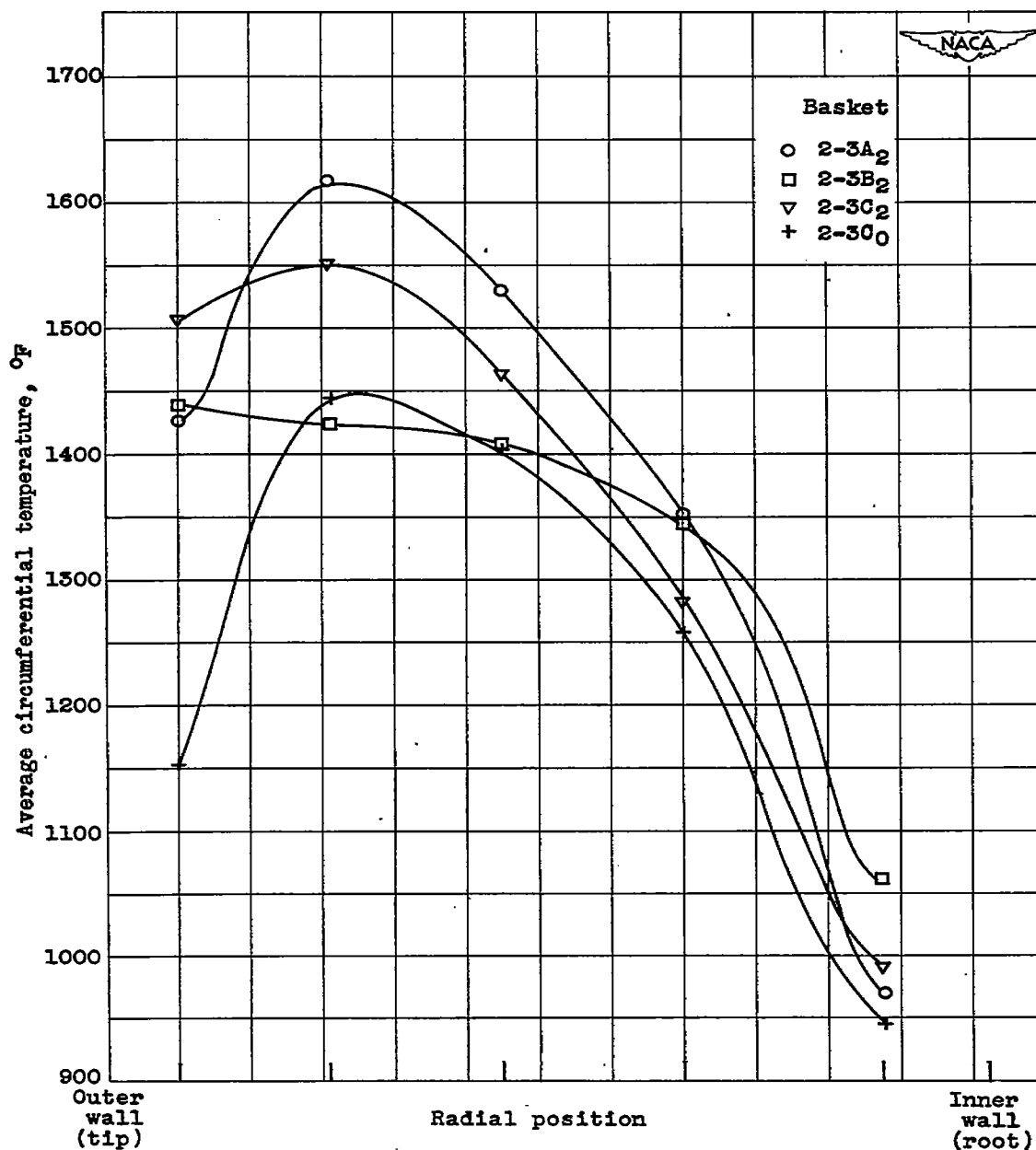combustor in series 2-2( )$_1$.

(e) Total-pressure loss shown as function of inlet-to-outlet density ratio. Operating conditions: altitude, 40,000 feet; engine speed, 17,400 rpm.

Figure 9. – Continued. Performance characteristics of one-sixth sector of annular turbojet combustor in series 2-2( )$_1$.
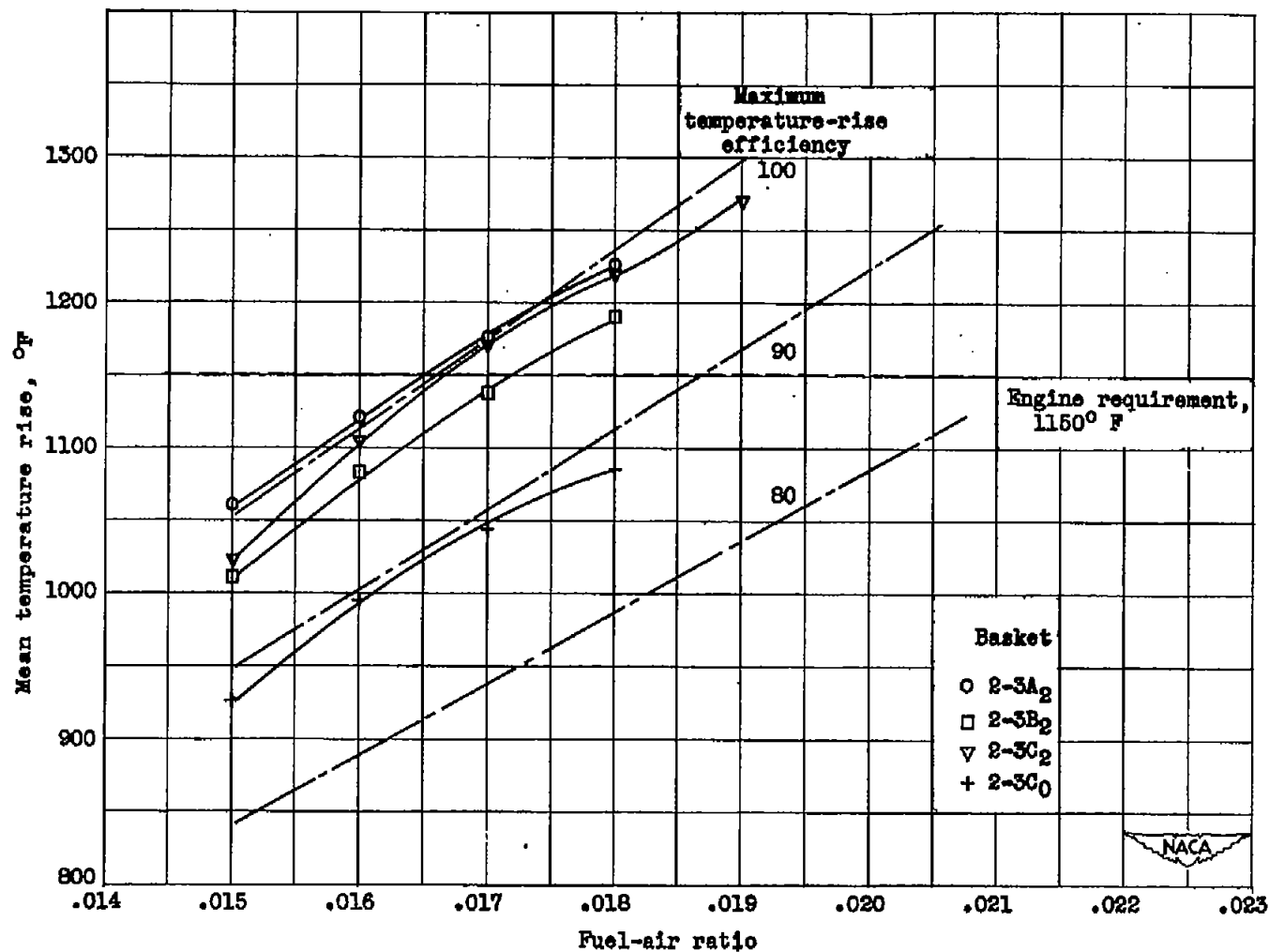
(f) Altitude operating limits. Shaded area shows band
        within which all operating limits fell for this series.

Figure 9. - Concluded. Performance characteristics of one-sixth
        sector of annular turbojet combustor in series 2-2( )$_1$.
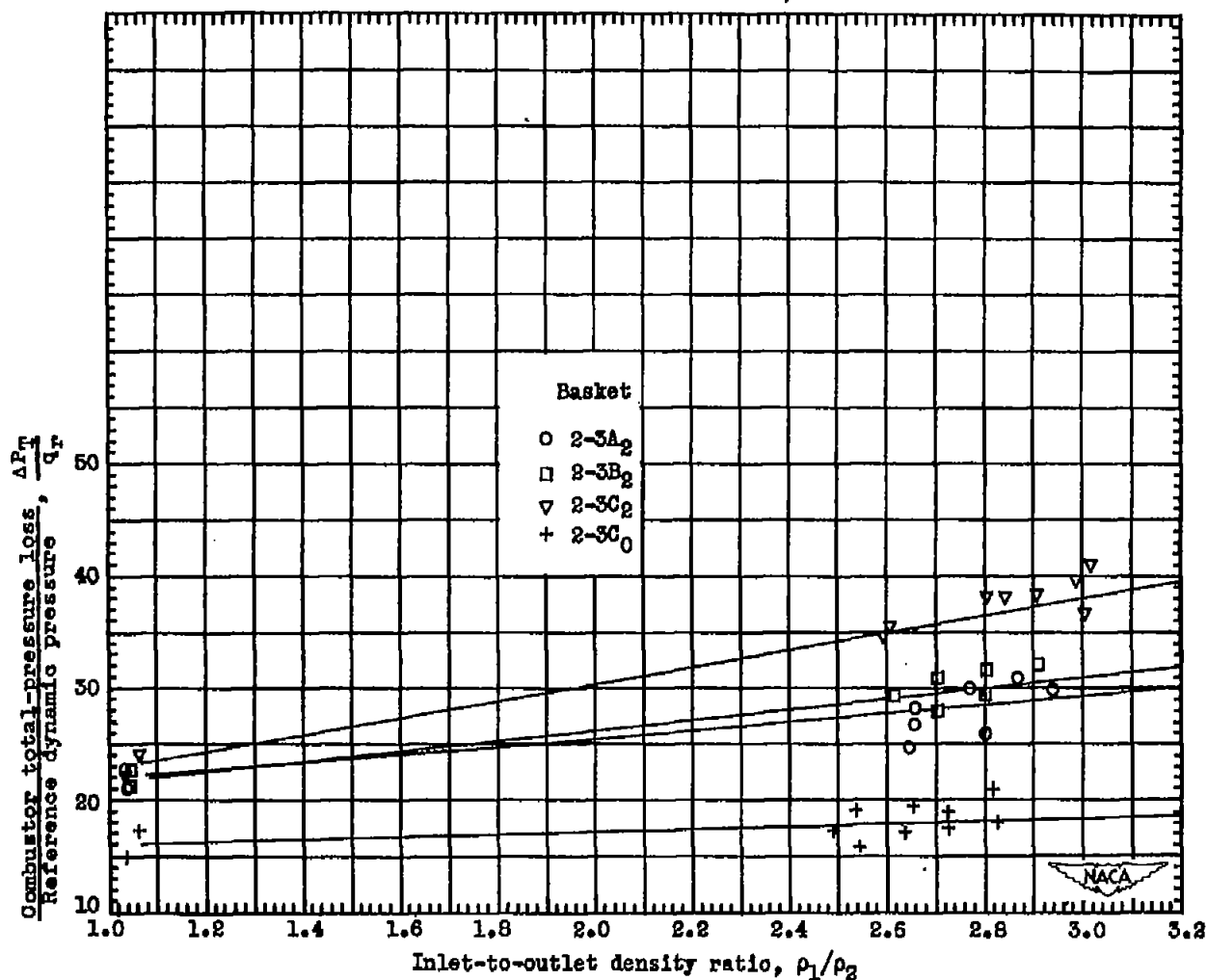
(a) Radial temperature distribution. Operating conditions:
     altitude, 40,000 feet; engine speed, 17,400 rpm; fuel-air
     ratio, 0.016.

Figure 10. – Performance characteristics of one-sixth sector of annular
             turbojet combustor in series 2-2( )$_2$.

(b) Radial temperature distribution. Operating conditions: altitude, 30,000 feet; engine speed, 17,400 rpm; fuel-air ratio, 0.016.

Figure 10. - Continued. Performance characteristics of one-sixth sector of annular turbojet combustor in series 2-2( )₂.
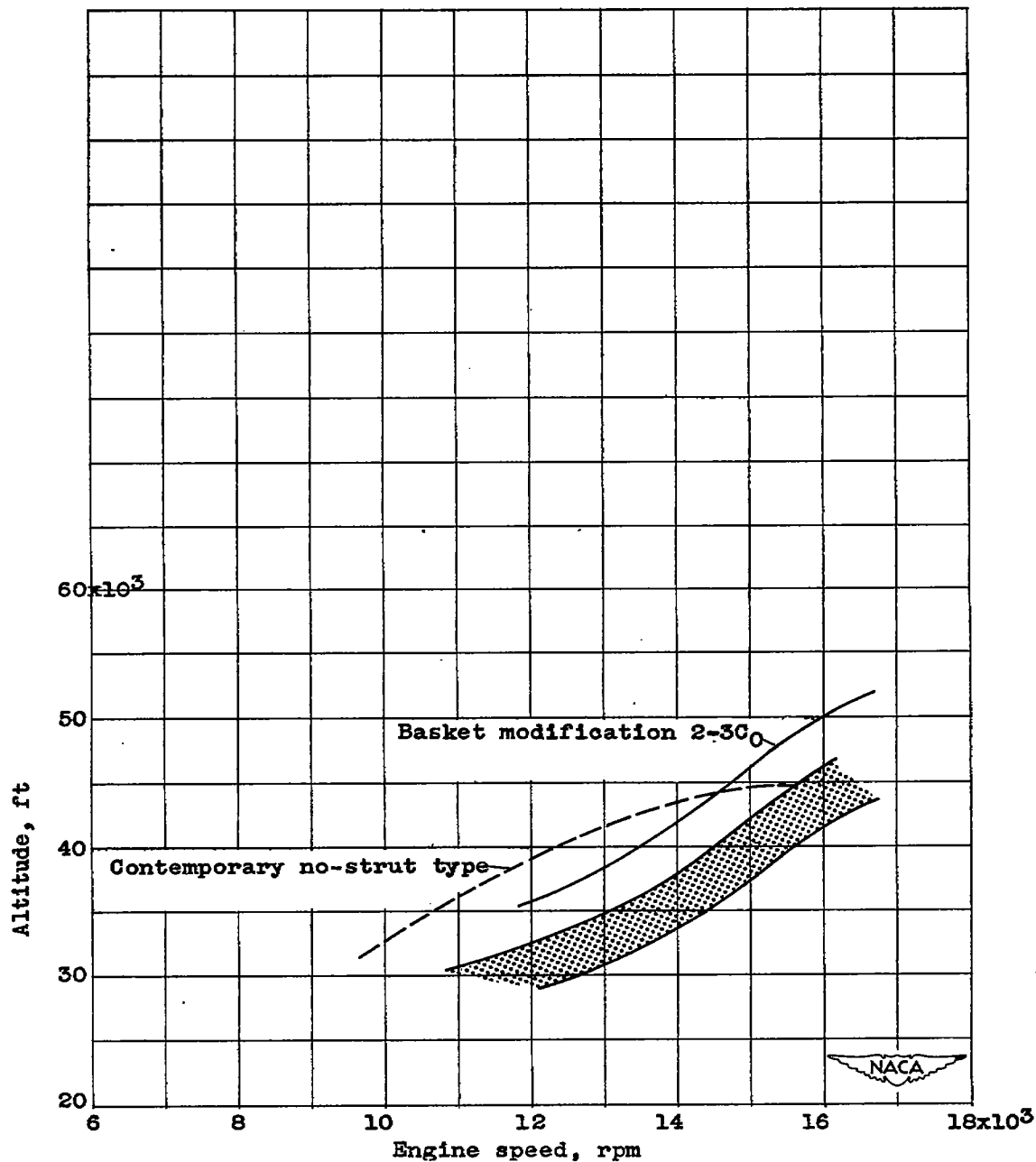
(c) Variation of mean temperature rise with fuel-air ratio. Operating conditions: altitude, 40,000 feet; engine speed, 17,400 rpm.

Figure 10. - Continued. Performance characteristics of one-sixth sector of annular turbojet combustor in series 2-2( )₂.

(d)   Total-pressure loss shown as function of inlet-to-outlet density ratio. Operating
conditions: altitude, 40,000 feet; engine speed, 17,400 rpm.

Figure 10. - Continued. Performance characteristics of one-sixth sector of annular turbojet
combustor in series 2-2( )$_2$.

1193

(e) Altitude operating limits. Shaded area shows band
within which all operating limits fell for this series.

Figure 10. - Concluded. Performance characteristics of one-sixth
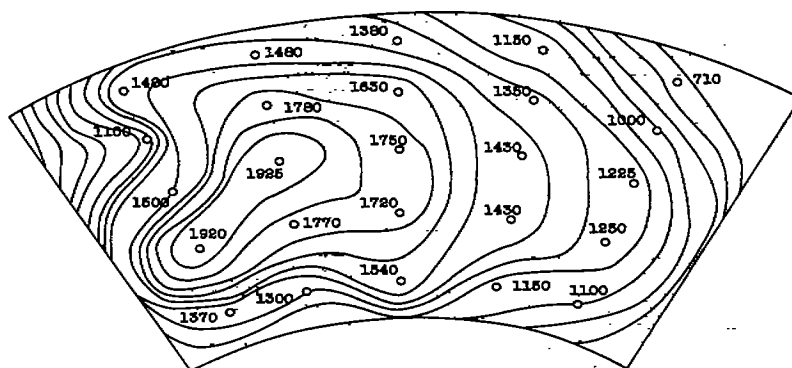sector of annular turbojet combustor in series 2-2( )$_2$.

1193

(a) Radial temperature distribution. Operating conditions:
       altitude, 40,000 feet; engine speed, 17,400 rpm; fuel-air
       ratio, 0.016.

Figure 11. - Performance characteristics of one-sixth sector of annular
                 turbojet combustor in series 2-3( )$_2$.

(b) Variation of mean temperature rise with fuel-air ratio. Operating conditions: altitude, 40,000 feet; engine speed, 17,400 rpm.

Figure 11. - Continued. Performance characteristics of one-sixth sector of annular turbojet combustor in series 2-3( )$_2$.

(c) Total-pressure loss shown as function of inlet-to-outlet density ratio. Operating conditions: altitude, 40,000 feet; engine speed, 17,400 rpm.

Figure 11. - Continued. Performance characteristics of one-sixth sector of annular turbojet combustor in series 2-3( )$_2$.

(d) Altitude operating limits. Shaded area shows band
     within which all operating limits fell for this series.

Figure 11. - Concluded. Performance characteristics of one-sixth
     sector of annular turbojet combustor in series 2-3( )$_2$.
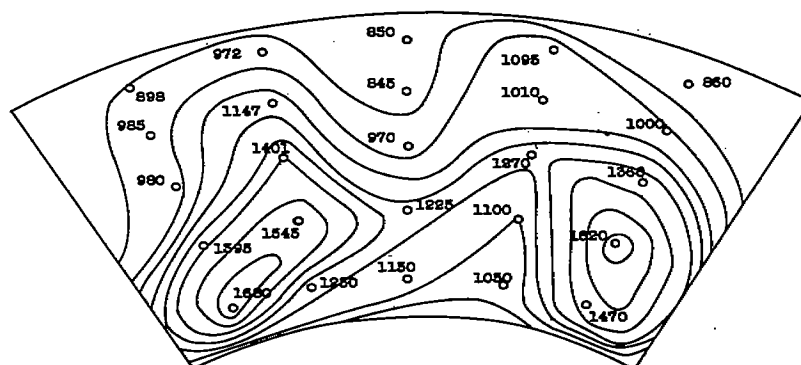
(a) Basket 1-1A$_1$.
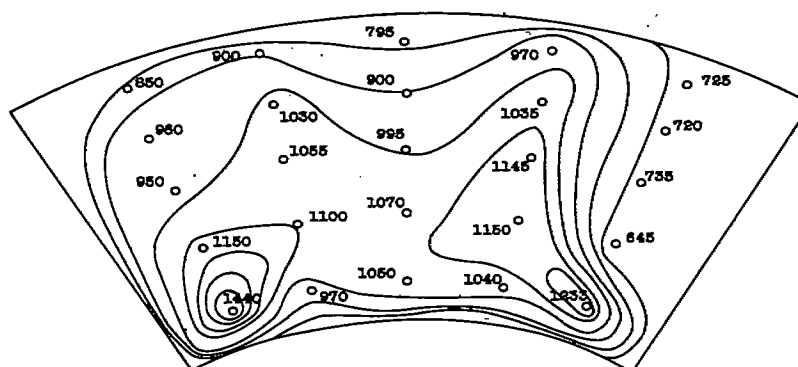
(b) Basket 1-1B$_1$.
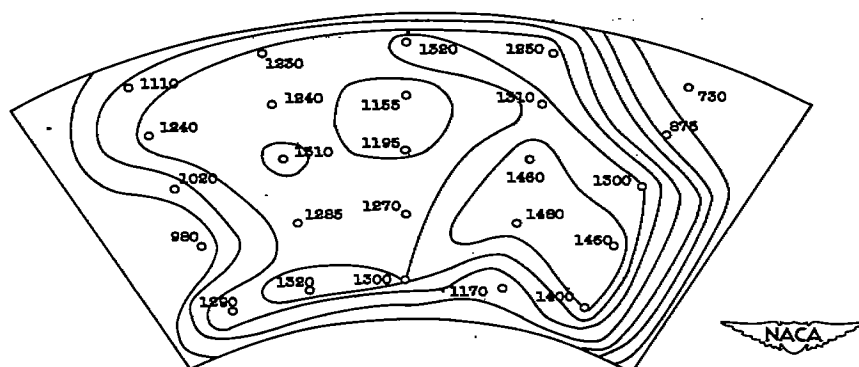
(c) Basket 1-1C$_1$.

Figure 12. - Temperature pattern at combustor outlet for one-sixth sector of annular turbojet combustor. Operating conditions: altitude, 40,000 feet; engine speed, 17,400 rpm; fuel-air ratio, 0.016. All temperatures are given in °F.
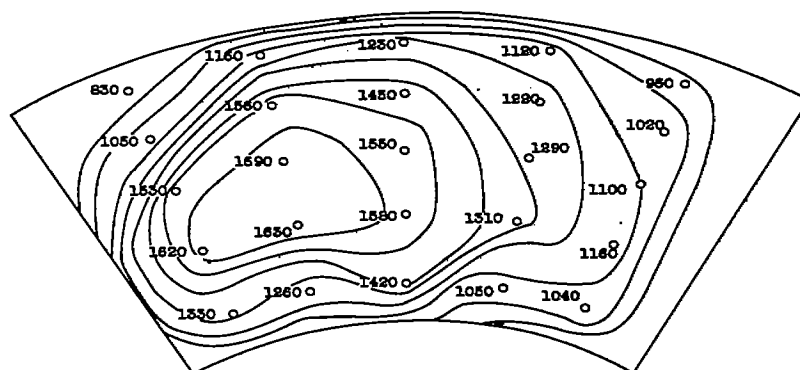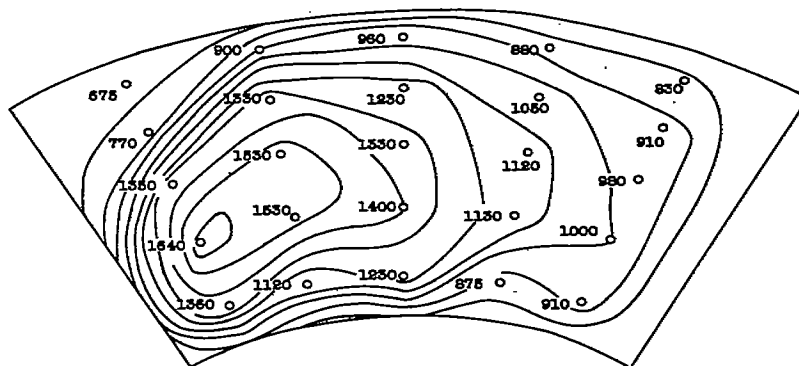
(d) Basket 1-2A$_1$.
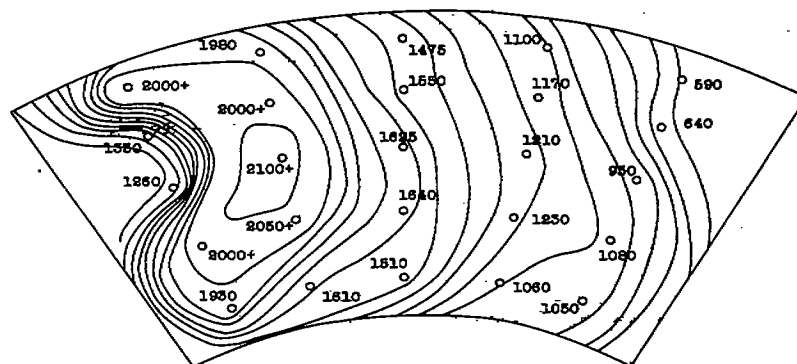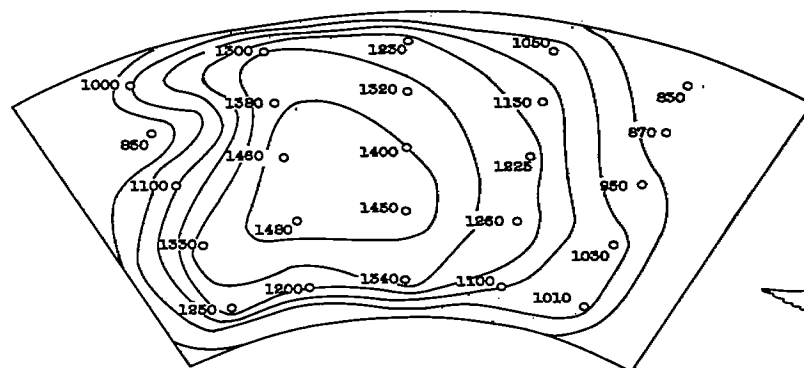
(e) Basket 1-2B$_1$.
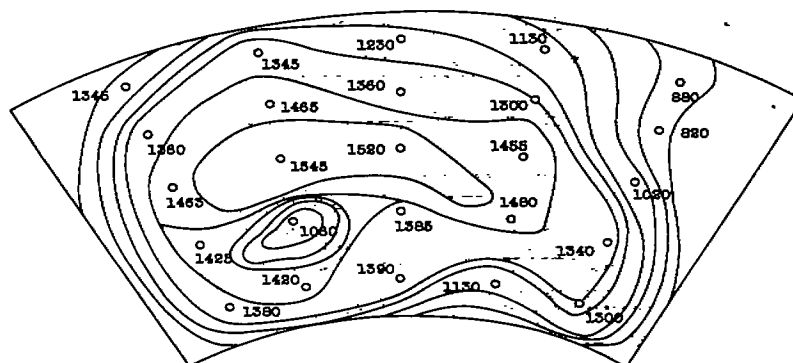
(f) Basket 1-2C$_1$.

Figure 12. - Continued. Temperature pattern at combustor outlet for one-sixth sector of
annular turbojet combustor. Operating conditions: altitude, 40,000 feet; engine
speed, 17,400 rpm; fuel-air ratio, 0.016. All temperatures are given in °F.

1193

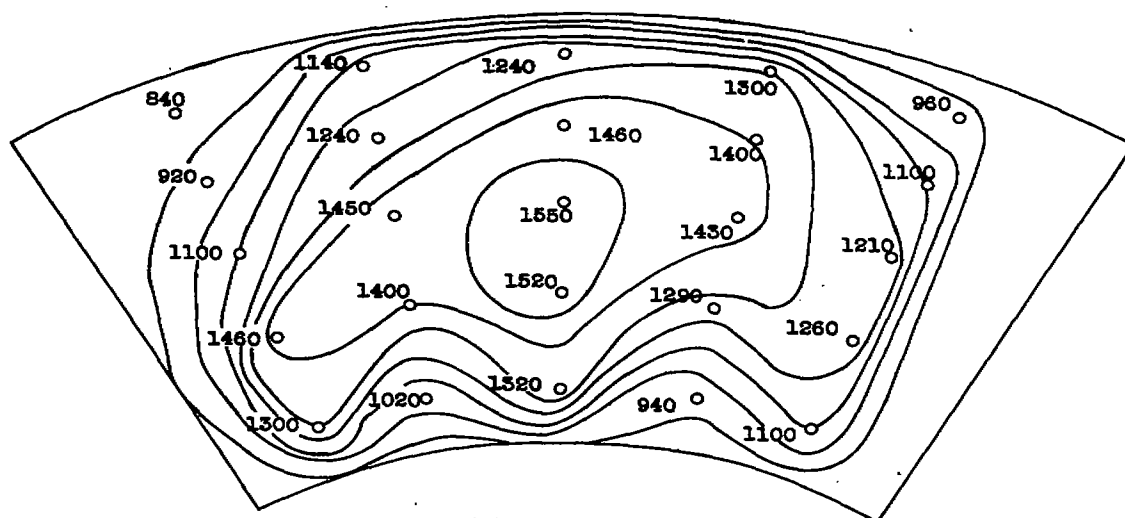

(g) Basket 2-2A$_1$.

(h) Basket 2-2B$_1$.
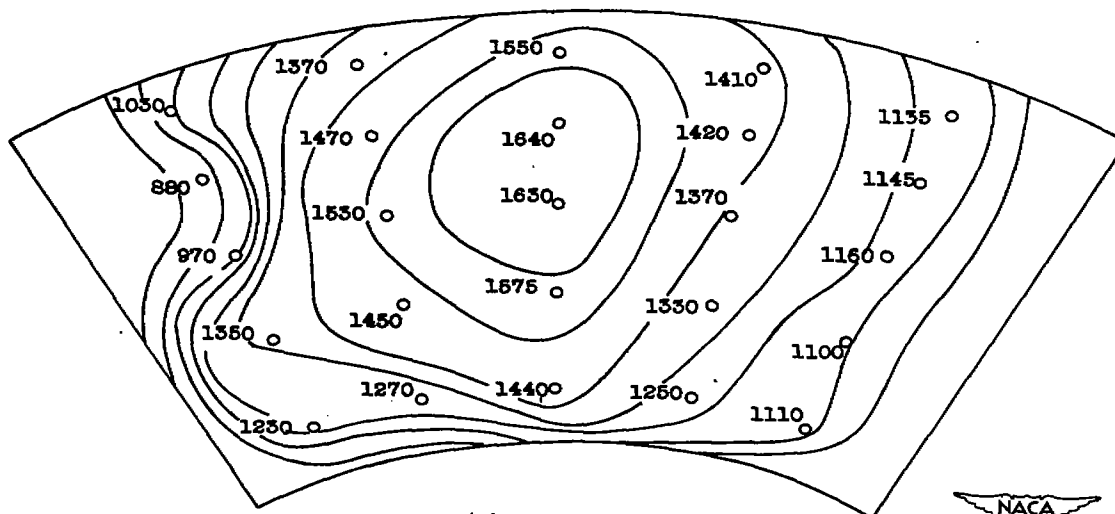

(i) Basket 2-2C$_1$.

Figure 12. - Continued.   Temperature pattern at combustor outlet for one-sixth sector of
annular turbojet combustor.   Operating conditions: altitude, 40,000 feet; engine
speed, 17,400 rpm; fuel-air ratio, 0.016.   All temperatures are given in °F.

1193

(j) Basket 2-2A$_2$.

(k) Basket 2-2C$_2$.

Figure 12. - Continued. Temperature pattern at combustor outlet for one-sixth sector of annular turbojet combustor. Operating conditions: altitude, 40,000 feet; engine speed, 17,400 rpm; fuel-air ratio, 0.016. All temperatures are given in °F.
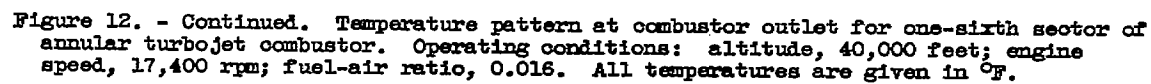
1193

(1) Basket 2-3A$_2$.
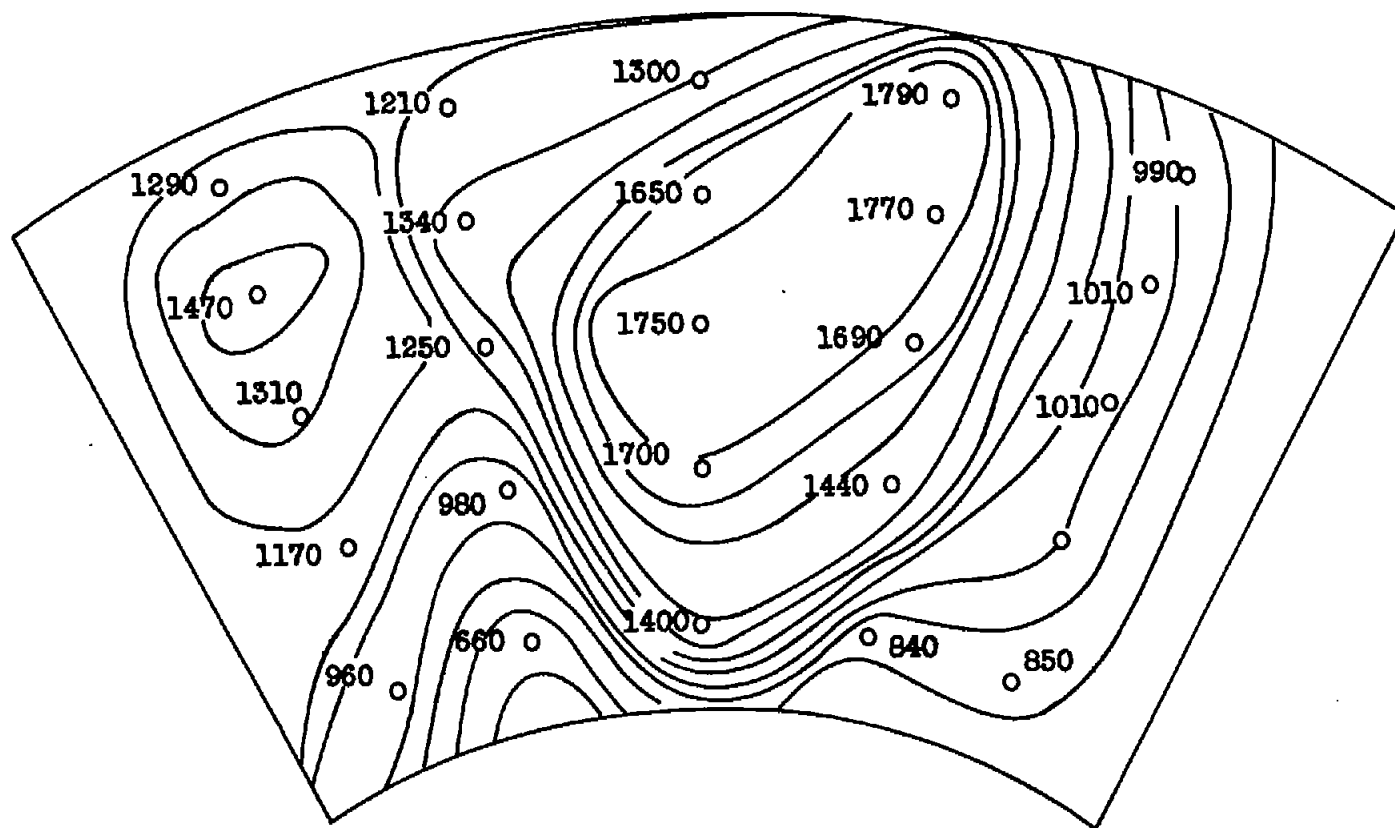

(m) Basket 2-3B$_2$.

(n) Basket 2-3C$_2$.

Figure 12. - Continued. Temperature pattern at combustor outlet for one-sixth sector of
annular turbojet combustor. Operating conditions: altitude, 40,000 feet; engine
speed, 17,400 rpm; fuel-air ratio, 0.016. All temperatures are given in °F.

(o) Basket 2-3C_0.

Figure 12. – Concluded. Temperature pattern at the combustor outlet for one-sixth sector of annular turbojet combustor. Operating conditions: altitude, 40,000 feet; engine speed, 17,400 rpm; fuel-air ratio, 0.016. All temperatures are given in ^{O}F.